AD-A131 384 MACH REFLECTION FLOW FIELDS ASSOCIATED WITH STRONG SHOCKS(U) AEROSPACE CORP EL SEGUNDO CA AEROPHYSICS LAB H MIRELS 25 JUL 83 TR-0083(3785)-1 SD-TR-83-50 1/1

UNCLASSIFIED F04701-82-C-0083 F/G 20/4 NL

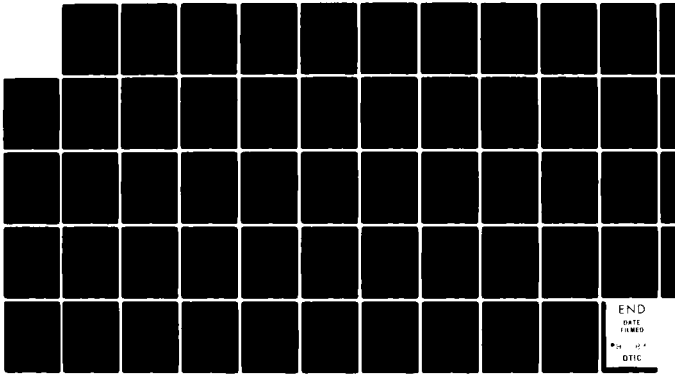

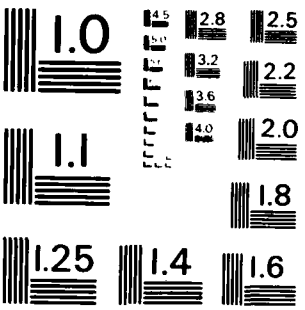

REPORT SD-TR-83-50

(12)

Mach Reflection Flow Fields Associated with Strong Shocks

H. MIRELS
Aerophysics Laboratory
Laboratory Operations
The Aerospace Corporation
El Segundo, Calif. 90245

25 July 1983

Prepared for
DEFENSE NUCLEAR AGENCY
Alexandria, Va. 22310

SPACE DIVISION
AIR FORCE SYSTEMS COMMAND
Los Angeles Air Force Station
P.O. Box 92960, Worldway Postal Center
Los Angeles, Calif. 90009

This report was submitted by The Aerospace Corporation, El Segundo, CA 90245, under Contract No. FO4701-82-C-0083 with the Space Division, P.O. Box 92960, Worldway Postal Center, Los Angeles, CA 90009. It was reviewed and approved for The Aerospace Corporation by W. P. Thompson, Jr., Director, Aerophysics Laboratory. Captain James A. Garcia, Det 1, AFSTC, was the Air Force project officer.

This report has been reviewed by the Public Affairs Office (PAS) and is releasable to the National Technical Information Service (NTIS). At NTIS, It will be available to the general public, including foreign nationals.

This technical report has been reviewed and is approved for publication. Publication of this report does not constitute Air Force approval of the report's findings or conclusions. It is published only for the exchange and stimulation of ideas.

James A. Garcia, Captain, USAF
Project Officer

Norman W. Lee, Jr., Colonel, USAF
Commander, Det 1, AFSTC

UNCLASSIFIED

SECURITY CLASSIFICATION OF THIS PAGE (When Data Entered)

REPORT DOCUMENTATION PAGE		READ INSTRUCTIONS BEFORE COMPLETING FORM
1. REPORT NUMBER SD-TR-83-50	2. GOVT ACCESSION NO. A131384	3. RECIPIENT'S CATALOG NUMBER
4. TITLE (and Subtitle) MACH REFLECTION FLOW FIELDS ASSOCIATED WITH STRONG SHOCKS		5. TYPE OF REPORT & PERIOD COVERED
		6. PERFORMING ORG. REPORT NUMBER TR-0083(3785)-1
7. AUTHOR(s) Harold Mirels		8. CONTRACT OR GRANT NUMBER(s) F04701-82-C-0083
9. PERFORMING ORGANIZATION NAME AND ADDRESS The Aerospace Corporation El Segundo, Calif. 90245		10. PROGRAM ELEMENT, PROJECT, TASK AREA & WORK UNIT NUMBERS
11. CONTROLLING OFFICE NAME AND ADDRESS Defense Nuclear Agency Alexandria, VA 22310		12. REPORT DATE 25 July 1983
		13. NUMBER OF PAGES 64
14. MONITORING AGENCY NAME & ADDRESS(if different from Controlling Office) Space Division Air Force Systems Command Los Angeles, Calif. 90009		15. SECURITY CLASS. (of this report) Unclassified
		15a. DECLASSIFICATION DOWNGRADING SCHEDULE

16. DISTRIBUTION STATEMENT (of this Report)

Approved for public release; distribution unlimited.

17. DISTRIBUTION STATEMENT (of the abstract entered in Block 20, if different from Report)

18. SUPPLEMENTARY NOTES

19. KEY WORDS (Continue on reverse side if necessary and identify by block number)

Blast waves
Shock reflection
Mach reflection
Height-of-burst effects
Recirculation

20. ABSTRACT (Continue on reverse side if necessary and identify by block number)

The Mach reflection associated with the passage of a shock wave over a wedge is treated in the limit of an ideal gas and a strong shock (i.e., $M_1^2 \gg 1$, where M_1 is the incident-shock Mach number). In this limit, flow properties are functions only of wedge angle θ and the ratio of specific heats γ. Numerical results are presented for $\gamma = 9/7$, 7/5, and 5/3. Wedge angles are noted at which the transition from regular to double-Mach, to complex-Mach, and to simple-Mach reflection occurs. Characteristic velocities in the recirculation region associated with Mach reflection are estimated. Local

DD FORM (FACSIMILE) 1473

UNCLASSIFIED

SECURITY CLASSIFICATION OF THIS PAGE (When Data Entered)

19. KEY WORDS (Continued)

20. ABSTRACT (Continued)

surface pressure maxima, at the upstream and downstream edge of the recirculation region, are also estimated. The scale of the recirculation region increases with decrease in γ, in accord with experimental observations. The wedge solution is used on a piecewise basis to estimate height-of-burst (HOB) flow fields. Normalized results are presented for HOB triple-point trajectory and surface pressure variation with range. The present results provide a convenient characterization of Mach reflection flow fields associated with both wedge and HOB flows. Validation of the HOB solution, however, is needed.

PREFACE

This work was partially supported by Defense Nuclear Agency (DNA) under the Air Force Space Division (AFSD). The computational support of Karen Foster is gratefully acknowledged.

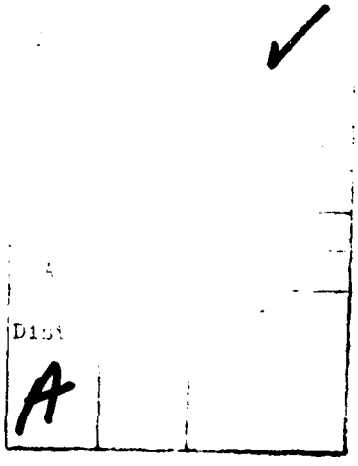

CONTENTS

FIGURES

TABLES

I. INTRODUCTION

The passage of a shock wave over a wedge results in either a regular or a Mach reflection. The Mach reflection flow field can be further divided into single-Mach, complex-Mach, and double-Mach reflections (Fig. 1). The conditions under which each of the latter flow regimes arise have been examined experimentally and analytically in Refs. 1, 2, and 3 and, more recently, in Ref. 4. Results from Ref. 4 that concern flow regimes are given in Fig. 2 and are discussed later.

The interaction with the ground of a blast wave initiated at altitude h also results in a Mach reflection for a portion of the flow duration (Fig. 3). This interaction, which is referred to as a "height-of-burst" (HOB) effect, is of interest in studies of the hardness of ground facilities to nuclear explosions. Numerical codes have been developed[5] that describe the transition from regular to Mach reflection in HOB flows. The numerical results appear to be in general agreement with experimental observations.

In the present study, we consider a wedge-induced Mach reflection flow field in the limit of a strong incident shock and an ideal inviscid gas. In this limit the flow field depends only on wedge angle and the ratio of specific heats γ. Results are tabulated for the flow in each of the five regions noted in Fig. 4. Regular reflection flow-field properties are included. These results are applied to estimate HOB flow fields. The present results provide a convenient characterization of Mach reflection flow fields associated with strong shocks for both wedge and HOB flows.

Results for $\gamma = 9/7$, 7/5, and 5/3 are presented in the body of this report. Results for $\gamma = 6/5$ appear in the Addendum.

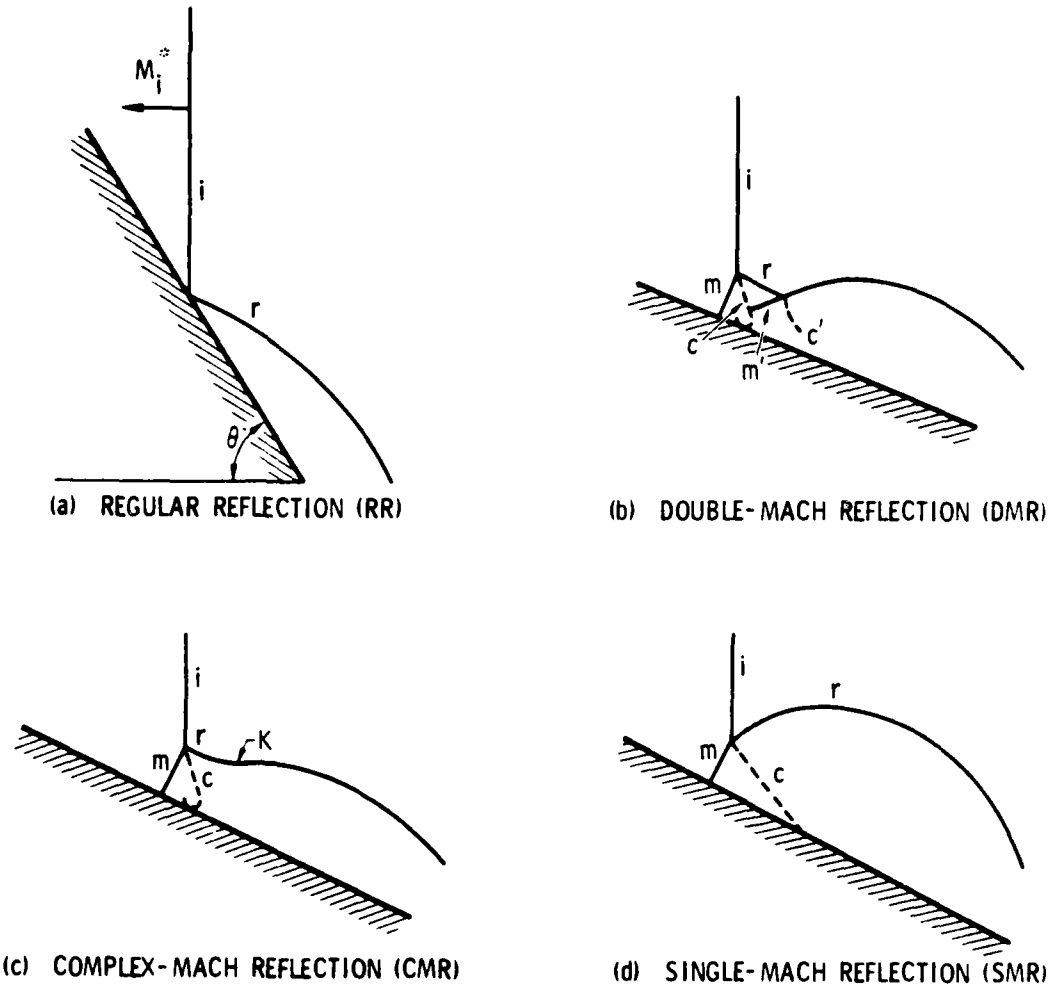

Fig. 1. Types of Oblique-Shock-Wave Reflections.
i = incident shock; r = reflected shock;
m = Mach stem; m′ = second Mach shock;
k = kink; c,c′ = contact surfaces (from Ref. 4)

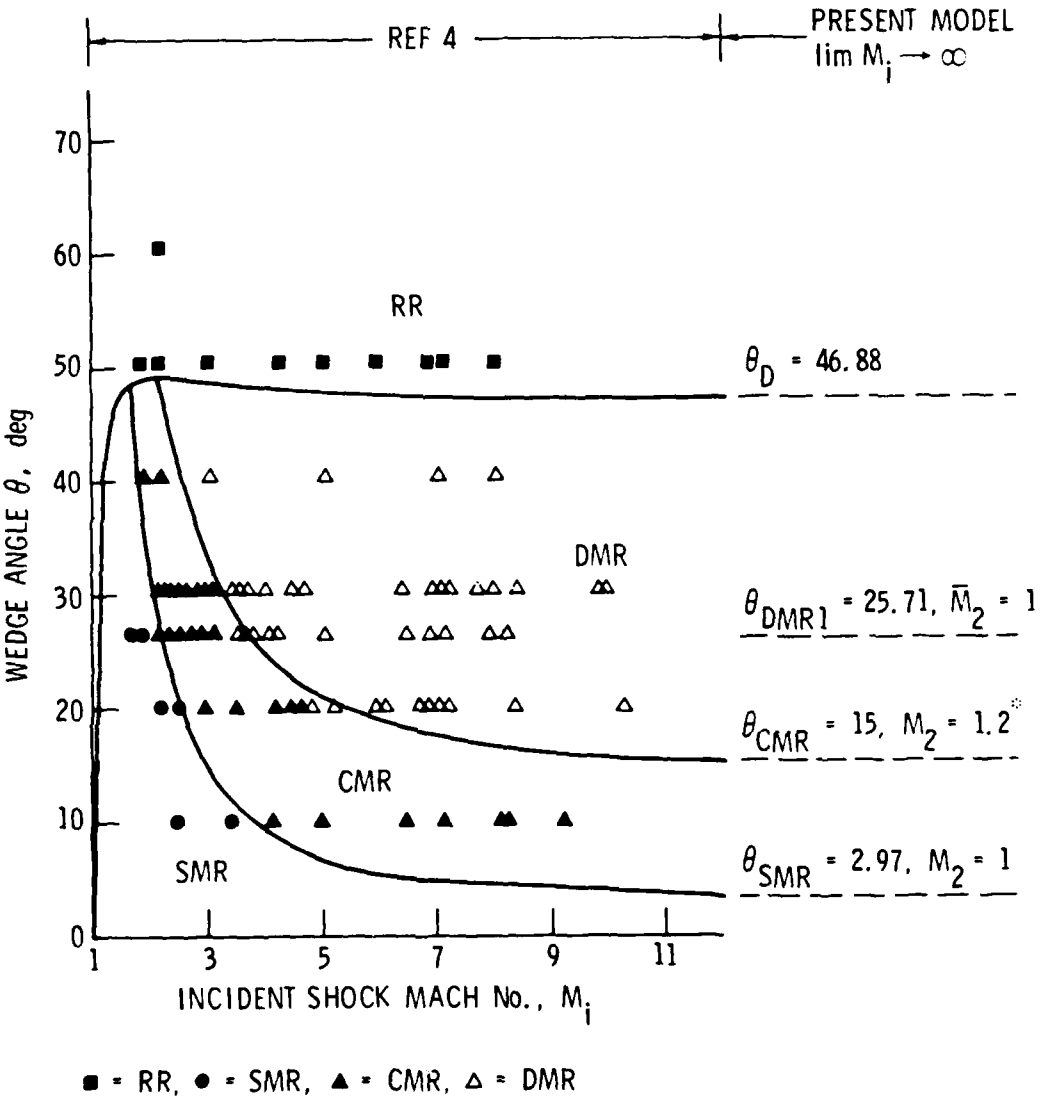

Fig. 2. Comparison of Predicted Reflection Regions and Experiment (perfect CO_2, γ = 1.290) (see Table 2)

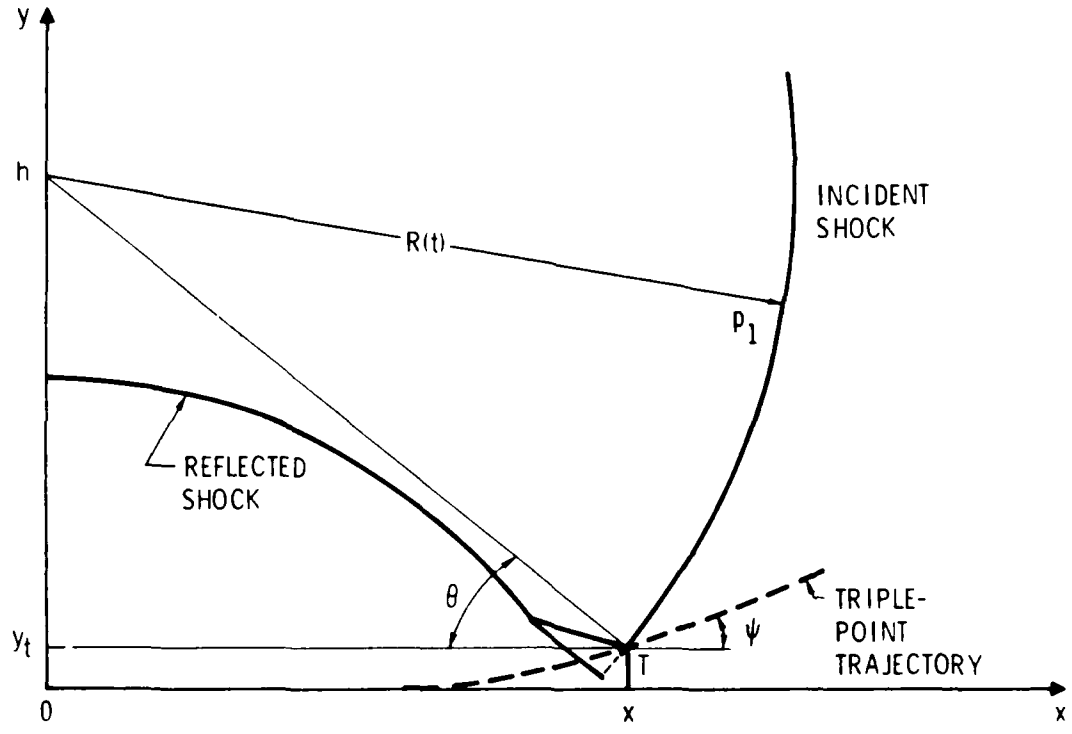

Fig. 3. Flow Field Associated with Blast Wave Initiated at Altitude h

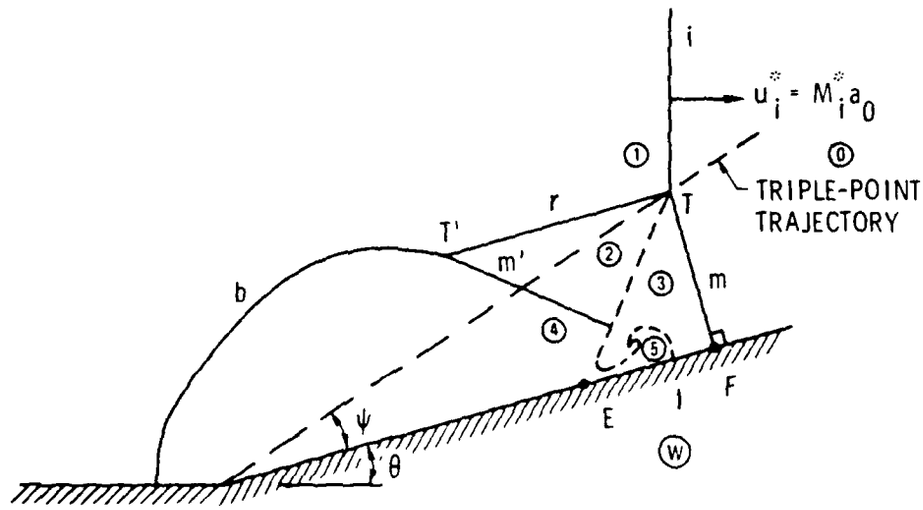

Fig. 4. Mach Reflection Flow Regions Associated with the Passage of Strong Incident Shock Past Wedge

II. DISCUSSION

Conditions across a strong shock in an ideal gas are noted in Appendix A. These are applied in Appendix B to determine the Mach reflection associated with passage of a strong shock over a wedge of angle θ. The case of regular reflection is treated in Appendix C. The application of these results to HOB is discussed in Appendix D. Numerical results are presented in Tables 1 through 4. These results are discussed herein.

The flow fields are considered in a variety of coordinate systems. Velocities in laboratory coordinates are denoted u^*. Velocities in coordinate systems wherein the points T, E, and F are stationary are denoted u, $\bar{u}$, and $\tilde{u}$, respectively, as is noted in Figs. 5 and 6. Here, point E is the intersection of the contact surface (assumed straight) with the wedge surface.

A. REGULAR REFLECTION

Figure 5 illustrates regular reflection in a coordinate system wherein point T is stationary. Flow properties are deduced in Appendix C and are listed in Table 1.

The flow in regions 1 and 2 corresponds to supersonic flow over an equivalent wedge of angle $\delta = (\pi/2) - \beta - \theta$, as noted in Fig. 5. The oblique shock that separates regions 1 and 2 can be either weak or strong (Ref. 6). The weak-shock solution appears to be physically realistic and is used herein. The equivalent wedge angle δ increases as θ is decreased. Ultimately, a value of θ, denoted θ_D, is reached below which no oblique shock solution is possible. The transition to Mach reflection is generally assumed to occur at θ_D (i.e., shock detachment criterion). The latter criterion has been used in Fig. 2 to define the regular reflection regime. For strong shocks, θ_D depends only on γ. Numerical results for θ_D are given in Table 2.

Table 1. Regular Reflection for the Case of Strong Incident Shock and Ideal Gas

γ	θ	M_1	β	$\frac{\rho_1}{\rho_0}$	$\frac{P_1}{M_1^2 P_0}$	M_2	δ	ω	$\frac{\rho_2}{\rho_1}$	$\frac{P_2}{P_1}$
9/7	90.00	∞	0.00	8.00	1.12	∞	0.00	.00	4.50	10.00
	85.00	30.48	0.63	8.00	1.12	20.39	4.37	1.26	4.49	9.94
	80.00	15.13	1.26	8.00	1.12	10.03	8.74	2.57	4.46	9.77
	75.00	9.96	1.92	8.00	1.12	6.50	13.08	3.99	4.40	9.49
	70.73	7.63	2.50	8.00	1.12	4.88	16.77	5.36	4.33	9.18
	70.00	7.33	2.60	8.00	1.12	4.67	17.40	5.61	4.32	9.12
	65.00	5.73	3.34	8.00	1.12	3.52	21.66	7.55	4.22	8.67
	60.00	4.63	4.13	8.00	1.12	2.70	25.87	10.00	4.10	8.16
	55.00	3.82	5.00	8.00	1.12	2.06	30.00	13.39	3.97	7.63
	50.00	3.20	5.99	8.00	1.12	1.49	34.01	18.99	3.86	7.20
	49.00	3.09	6.20	8.00	1.12	1.37	34.80	20.78	3.85	7.16
	48.00	2.98	6.42	8.00	1.12	1.23	35.58	23.18	3.85	7.18
	47.00	2.88	6.65	8.00	1.12	1.03	36.35	27.75	3.91	7.42
	46.88	2.87	6.68	8.00	1.12	0.95	36.45	30.12	3.98	7.66
7/5	90.00	∞	0.00	6.00	1.17	∞	0.00	.00	3.50	8.00
	85.00	25.92	0.84	6.00	1.17	17.09	4.16	1.68	3.49	7.96
	80.00	12.87	1.68	6.00	1.17	8.40	8.32	3.43	3.47	7.84
	75.00	8.47	2.56	6.00	1.17	5.43	12.44	5.33	3.43	7.64
	70.00	6.24	3.47	6.00	1.17	3.89	16.53	7.51	3.38	7.38
	68.23	5.69	3.81	6.00	1.17	3.51	17.96	8.37	3.36	7.27
	65.00	4.88	4.44	6.00	1.17	2.92	20.56	10.13	3.32	7.06
	60.00	3.95	5.50	6.00	1.17	2.22	24.50	13.53	3.25	6.73
	55.00	3.26	6.66	6.00	1.17	1.65	28.34	18.52	3.19	6.44
	54.00	3.14	6.90	6.00	1.17	1.55	29.10	19.90	3.18	6.40
	53.00	3.03	7.16	6.00	1.17	1.44	29.84	21.51	3.17	6.38
	52.00	2.93	7.42	6.00	1.17	1.32	30.58	23.50	3.17	6.39
	51.00	2.83	7.69	6.00	1.17	1.19	31.31	26.20	3.19	6.46
	50.03	2.73	7.95	6.00	1.17	0.95	32.02	32.79	3.30	6.96
5/3	90.00	∞	0.00	4.00	1.25	∞	0.00	.00	2.50	6.00
	85.00	20.45	1.25	4.00	1.25	13.15	3.75	2.52	2.50	5.98
	80.00	10.15	2.52	4.00	1.25	6.45	7.48	5.15	2.49	5.91
	75.00	6.69	3.83	4.00	1.25	4.16	11.17	8.02	2.47	5.80
	70.00	4.94	5.20	4.00	1.25	2.97	14.80	11.34	2.45	5.66
	65.00	3.86	6.65	4.00	1.25	2.21	18.35	15.43	2.42	5.51
	64.78	3.82	6.71	4.00	1.25	2.18	18.50	15.64	2.42	5.51
	60.00	3.13	8.21	4.00	1.25	1.64	21.79	21.09	2.41	5.42
	59.00	3.01	8.54	4.00	1.25	1.54	22.46	22.58	2.41	5.42
	58.00	2.90	8.88	4.00	1.25	1.43	23.12	24.29	2.41	5.44
	57.00	2.79	9.22	4.00	1.25	1.33	23.78	26.32	2.42	5.48
	56.00	2.69	9.57	4.00	1.25	1.21	24.43	28.92	2.43	5.57
	55.00	2.59	9.93	4.00	1.25	1.07	25.07	33.04	2.47	5.81
	54.66	2.56	10.05	4.00	1.25	0.95	25.29	37.25	2.53	6.21

Table 2. Wedge Angles at Which Mach Reflection Flow-Field Transitions Occur for the Case of Strong Shock and Ideal Gas

	θ			
	θ_D	θ_{DMR1}	θ_{CMR}	θ_{SMR}
	RR → DMR	$\bar{M}_2 = 1$	DMR → CMR	CMR → SMR
γ	$M_2 > \bar{M}_2 > 1$	$M_2 \doteq 1.6$	$M_2 = 1.3$	$M_2 = 1$
1.10	37.34			
1.20	43.54	20.49	14.4	1.19
9/7	46.88	25.71	18.5[a]	2.97
1.30	47.34			
1.40	50.03	32.36	23.7	5.89
1.50	52.09			
1.60	53.73			
5/3	54.66	47.94	35.2	14.33

[a]Reference 4 appears to have used the value $\theta_{CMR} = 15°$ ($M_2 = 1.2$) for $\gamma = 9/7$ (see Fig. 2).

Table 3a. Mach Reflection for the Case of Strong Shock and Ideal Gas, $\gamma = 9/7$

		Region 1				Region 2				
θ	ϕ	M_1	ξ	$\frac{\rho_1}{\rho_0}$	$\frac{p_1}{M_1^2 p_0}$	M_2	ξ	ω	$\frac{\rho_2}{\rho_1}$	$\frac{p_2}{p_1}$
70.728	0.000	7.634	2.503	8.000	1.125	4.880	16.769	5.362	4.333	9.180
70.000	0.090	7.370	2.592	8.000	1.125	4.789	16.687	5.545	4.210	8.623
67.500	0.402	6.576	2.905	8.000	1.125	4.489	16.385	6.224	3.818	7.066
65.000	0.717	5.920	3.228	8.000	1.125	4.206	16.052	6.983	3.472	5.912
62.500	1.038	5.368	3.560	8.000	1.125	3.940	15.690	7.823	3.167	5.035
60.000	1.366	4.895	3.904	8.000	1.125	3.692	15.299	8.749	2.900	4.352
57.500	1.700	4.486	4.261	8.000	1.125	3.460	14.879	9.764	2.666	3.811
55.000	2.044	4.127	4.633	8.000	1.125	3.244	14.431	10.872	2.461	3.375
52.500	2.398	3.809	5.021	8.000	1.125	3.043	13.956	12.080	2.283	3.019
50.000	2.764	3.524	5.427	8.000	1.125	2.855	13.453	13.392	2.126	2.725
47.500	3.144	3.269	5.853	8.000	1.125	2.680	12.924	14.817	1.988	2.479
46.880	3.241	3.209	5.962	8.000	1.125	2.638	12.789	15.189	1.957	2.425
45.000	3.540	3.037	6.302	8.000	1.125	2.516	12.369	16.364	1.867	2.272
42.500	3.953	2.825	6.776	8.000	1.125	2.362	11.788	18.041	1.760	2.097
40.000	4.387	2.631	7.277	8.000	1.125	2.218	11.182	19.862	1.666	1.947
37.500	4.845	2.453	7.810	8.000	1.125	2.083	10.551	21.839	1.583	1.818
35.000	5.329	2.288	8.376	8.000	1.125	1.956	9.894	23.990	1.509	1.706
32.500	5.843	2.135	8.980	8.000	1.125	1.836	9.211	26.333	1.444	1.609
30.000	6.393	1.994	9.625	8.000	1.125	1.725	8.504	28.892	1.385	1.524
27.500	6.982	1.862	10.315	8.000	1.125	1.620	7.770	31.693	1.333	1.450
25.000	7.618	1.739	11.052	8.000	1.125	1.522	7.011	34.765	1.287	1.385
22.500	8.308	1.625	11.839	8.000	1.125	1.431	6.226	38.147	1.246	1.327
20.000	9.059	1.519	12.678	8.000	1.125	1.346	5.417	41.876	1.209	1.276
17.500	9.884	1.421	13.567	8.000	1.125	1.269	4.588	46.000	1.175	1.231
15.000	10.796	1.331	14.500	8.000	1.125	1.199	3.745	50.566	1.145	1.190
12.500	11.811	1.250	15.466	8.000	1.125	1.138	2.902	55.627	1.117	1.154
10.000	12.952	1.177	16.445	8.000	1.125	1.085	2.080	61.232	1.092	1.120
7.500	14.245	1.115	17.401	8.000	1.125	1.043	1.314	67.426	1.068	1.089
5.000	15.726	1.063	18.281	8.000	1.125	1.013	0.657	74.245	1.046	1.059
2.500	17.443	1.023	19.009	8.000	1.125	0.997	0.185	81.733	1.023	1.030
1.000	18.616	1.007	19.327	8.000	1.125	0.996	0.032	86.585	1.009	1.012

Table 3a. Mach Reflection for the Case of Strong Shock and Ideal Gas, $\gamma = 9/7$ (Continued)

			Region 3			Region 4			
θ	M_3	α	$\frac{\rho_3}{\rho_0}$	$\frac{P_3}{M_1^2 P_0}$	$\bar{M}_2$	$\frac{\rho_4}{\rho_2}$	$\frac{P_4}{P_2}$	$\frac{P_{0,4}}{P_3}$	$\frac{P_4}{P_1}$
70.728	0.333	89.999	8.000	10.327	4.186	5.716	19.587	21.636	179.809
70.000	0.333	89.279	8.000	9.701	4.105	5.653	18.837	20.831	162.429
67.500	0.334	86.790	8.000	7.949	3.837	5.422	16.437	18.256	116.149
65.000	0.335	84.280	8.000	6.651	3.582	5.176	14.309	15.973	84.595
62.500	0.337	81.750	8.000	5.664	3.341	4.917	12.433	13.960	62.593
60.000	0.339	79.203	8.000	4.896	3.114	4.646	10.786	12.194	46.939
57.500	0.343	76.640	8.000	4.287	2.901	4.367	9.343	10.647	35.604
55.000	0.347	74.064	8.000	3.797	2.701	4.082	8.080	9.293	27.268
52.500	0.352	71.477	8.000	3.396	2.512	3.793	6.974	8.109	21.053
50.000	0.357	68.880	8.000	3.065	2.334	3.501	6.004	7.072	16.361
47.500	0.364	66.277	8.000	2.789	2.166	3.211	5.154	6.163	12.779
46.880	0.366	65.631	8.000	2.728	2.126	3.139	4.960	5.956	12.027
45.000	0.372	63.671	8.000	2.556	2.007	2.923	4.408	5.366	10.017
42.500	0.381	61.064	8.000	2.359	1.856	2.639	3.752	4.668	7.868
40.000	0.391	58.459	8.000	2.190	1.713	2.363	3.176	4.056	6.182
37.500	0.403	55.860	8.000	2.045	1.576	2.095	2.669	3.520	4.851
35.000	0.416	53.270	8.000	1.919	1.445	1.837	2.223	3.052	3.792
32.500	0.431	50.692	8.000	1.810	1.319	1.592	1.832	2.646	2.947
30.000	0.448	48.129	8.000	1.715	1.198	1.361	1.489	2.297	2.269
27.500	0.467	45.585	8.000	1.631	1.081	1.144	1.189	2.002	1.725
25.000	0.488	43.062	8.000	1.558	0.968	1.000	1.000	1.760	1.385
22.500	0.513	40.565	8.000	1.493	0.859	1.000	1.000	1.569	1.327
20.000	0.540	38.095	8.000	1.436	0.752	1.000	1.000	1.419	1.276
17.500	0.572	35.654	8.000	1.385	0.649	1.000	1.000	1.301	1.231
15.000	0.608	33.245	8.000	1.339	0.549	1.000	1.000	1.209	1.190
12.500	0.650	30.868	8.000	1.298	0.451	1.000	1.000	1.137	1.154
10.000	0.698	28.525	8.000	1.260	0.356	1.000	1.000	1.084	1.120
7.500	0.755	26.214	8.000	1.225	0.263	1.000	1.000	1.045	1.089
5.000	0.822	23.938	8.000	1.192	0.173	1.000	1.000	1.019	1.059
2.500	0.902	21.694	8.000	1.159	0.085	1.000	1.000	1.005	1.030
1.000	0.958	20.359	8.000	1.139	0.034	1.000	1.000	1.001	1.012

Table 3a. Mach Reflection for the Case of Strong Shock and Ideal Gas, $\gamma = 9/7$ (Continued)

	Region 5					Interfaces			
θ	$\bar{M}_5$	$\frac{\rho_5}{\rho_2}$	$\frac{\bar{u}_5}{u_1}$	$\frac{\tilde{u}_5}{u_1}$	$\frac{\bar{u}_I}{\bar{u}_m}$	$\frac{p_I}{p_3}$	$\frac{\bar{u}_m}{u_1}$	$\frac{\bar{u}_w}{u_1}$	$\frac{\tilde{u}_w}{u_1}$
70.728	2.619	1.769	0.459	0.080	0.891	1.058	0.379	2.651	3.030
70.000	2.597	1.736	0.469	0.102	0.933	1.064	0.367	2.569	2.937
67.500	2.520	1.627	0.499	0.167	1.072	1.085	0.332	2.326	2.658
65.000	2.441	1.530	0.524	0.220	1.203	1.108	0.304	2.128	2.431
62.500	2.361	1.444	0.545	0.265	1.325	1.132	0.280	1.963	2.244
60.000	2.281	1.368	0.564	0.303	1.440	1.157	0.261	1.825	2.086
57.500	2.200	1.302	0.581	0.337	1.550	1.183	0.244	1.708	1.952
55.000	2.119	1.244	0.597	0.367	1.653	1.211	0.230	1.607	1.837
52.500	2.036	1.194	0.611	0.394	1.752	1.239	0.217	1.520	1.738
50.000	1.952	1.151	0.625	0.418	1.847	1.268	0.206	1.444	1.651
47.500	1.867	1.115	0.638	0.441	1.938	1.298	0.197	1.378	1.575
46.880	1.846	1.107	0.641	0.446	1.960	1.305	0.195	1.363	1.557
45.000	1.780	1.085	0.650	0.461	2.025	1.328	0.188	1.319	1.507
42.500	1.691	1.060	0.661	0.480	2.110	1.360	0.181	1.267	1.448
40.000	1.598	1.040	0.672	0.498	2.190	1.391	0.174	1.221	1.395
37.500	1.503	1.024	0.682	0.513	2.265	1.422	0.169	1.180	1.348
35.000	1.404	1.013	0.689	0.526	2.334	1.453	0.163	1.143	1.306
32.500	1.300	1.006	0.695	0.536	2.395	1.480	0.159	1.110	1.268
30.000	1.192	1.002	0.697	0.543	2.444	1.503	0.154	1.080	1.235
27.500	1.080	1.000	0.696	0.546	2.479	1.520	0.151	1.054	1.204
25.000	0.968	1.000	0.692	0.545	2.502	1.531	0.147	1.030	1.177
22.500	0.859	1.000	0.687	0.543	2.518	1.540	0.144	1.008	1.152
20.000	0.752	1.000	0.682	0.541	2.529	1.545	0.141	0.989	1.130
17.500	0.649	1.000	0.676	0.537	2.536	1.549	0.139	0.971	1.109
15.000	0.549	1.000	0.670	0.533	2.538	1.550	0.136	0.955	1.091
12.500	0.451	1.000	0.663	0.529	2.538	1.550	0.134	0.940	1.074
10.000	0.356	1.000	0.656	0.524	2.535	1.548	0.132	0.926	1.058
7.500	0.263	1.000	0.649	0.519	2.530	1.546	0.130	0.913	1.044
5.000	0.173	1.000	0.642	0.514	2.524	1.543	0.129	0.901	1.029
2.500	0.085	1.000	0.635	0.508	2.515	1.538	0.127	0.888	1.015
1.000	0.034	1.000	0.629	0.503	2.508	1.534	0.126	0.880	1.006

Table 3b. Mach Reflection for the Case of Strong Shock and Ideal Gas, $\gamma = 7/5$

		Region 1				Region 2				
θ	ω	M_1	ξ	$\frac{\rho_1}{\rho_0}$	$\frac{p_1}{M_1^2 p_0}$	M_2	ξ	ω	$\frac{\rho_2}{\rho_1}$	$\frac{p_2}{p_1}$
68.231	0.000	5.691	3.808	6.000	1.167	3.506	17.961	8.374	3.363	7.271
65.000	0.532	4.998	4.337	6.000	1.167	3.262	17.473	9.500	3.041	5.829
62.500	0.950	4.554	4.760	6.000	1.167	3.083	17.057	10.476	2.819	5.004
60.000	1.375	4.172	5.198	6.000	1.167	2.912	16.608	11.545	2.620	4.354
57.500	1.808	3.839	5.650	6.000	1.167	2.751	16.128	12.712	2.441	3.834
55.000	2.250	3.546	6.119	6.000	1.167	2.598	15.616	13.982	2.281	3.412
52.500	2.704	3.285	6.607	6.000	1.167	2.454	15.072	15.361	2.139	3.064
50.030	3.165	3.054	7.108	6.000	1.167	2.320	14.506	16.835	2.013	2.778
47.500	3.653	2.841	7.645	6.000	1.167	2.191	13.895	18.467	1.898	2.531
45.000	4.153	2.650	8.200	6.000	1.167	2.070	13.261	20.211	1.796	2.325
42.500	4.672	2.476	8.782	6.000	1.167	1.957	12.598	22.094	1.705	2.150
40.000	5.214	2.316	9.393	6.000	1.167	1.850	11.906	24.126	1.624	1.998
37.500	5.782	2.169	10.036	6.000	1.167	1.749	11.185	26.322	1.551	1.868
35.000	6.379	2.033	10.713	6.000	1.167	1.655	10.435	28.694	1.486	1.754
32.500	7.009	1.908	11.426	6.000	1.167	1.567	9.657	31.259	1.428	1.655
30.000	7.678	1.792	12.178	6.000	1.167	1.484	8.852	34.035	1.375	1.568
27.500	8.391	1.684	12.970	6.000	1.167	1.406	8.019	37.042	1.328	1.491
25.000	9.154	1.584	13.802	6.000	1.167	1.334	7.162	40.303	1.285	1.423
22.500	9.976	1.492	14.674	6.000	1.167	1.268	6.284	43.839	1.246	1.363
20.000	10.864	1.407	15.582	6.000	1.167	1.208	5.388	47.674	1.211	1.309
17.500	11.831	1.329	16.521	6.000	1.167	1.154	4.485	51.832	1.179	1.260
15.000	12.890	1.258	17.480	6.000	1.167	1.106	3.586	56.329	1.150	1.216
12.500	14.055	1.195	18.443	6.000	1.167	1.066	2.711	61.178	1.123	1.176
10.000	15.345	1.139	19.386	6.000	1.167	1.033	1.888	66.377	1.097	1.139
7.500	16.780	1.091	20.277	6.000	1.167	1.009	1.153	71.909	1.073	1.103
5.000	18.385	1.051	21.077	6.000	1.167	0.995	0.554	77.736	1.049	1.069
2.500	20.185	1.021	21.738	6.000	1.167	0.991	0.149	83.794	1.025	1.035
1.000	21.370	1.007	22.046	6.000	1.167	0.995	0.025	87.505	1.010	1.014

Table 3b. Mach Reflection for the Case of Strong Shock and Ideal Gas, $\gamma = 7/5$ (Continued)

	Region 3				Region 4				
θ	M_3	α	$\frac{\rho_3}{\rho_0}$	$\frac{P_3}{M_1^2 P_0}$	$\bar{M}_2$	$\frac{\rho_4}{\rho_2}$	$\frac{P_4}{P_2}$	$\frac{P_{s,4}}{P_3}$	$\frac{P_4}{P_1}$
68.231	0.378	90.000	6.000	8.482	4.199	4.675	20.406	23.171	148.364
65.000	0.379	86.810	6.000	6.800	2.602	3.451	7.732	9.194	45.068
62.500	0.380	84.317	6.000	5.838	2.445	3.267	6.808	8.177	34.065
60.000	0.382	81.806	6.000	5.080	2.294	3.077	5.974	7.259	26.012
57.500	0.385	79.278	6.000	4.473	2.150	2.882	5.225	6.436	20.034
55.000	0.388	76.735	6.000	3.980	2.012	2.684	4.554	5.700	15.538
52.500	0.393	74.179	6.000	3.575	1.880	2.484	3.955	5.044	12.119
50.000	0.398	71.644	6.000	3.241	1.755	2.287	3.427	4.466	9.519
47.500	0.405	69.040	6.000	2.953	1.633	2.087	2.944	3.940	7.454
45.000	0.412	66.461	6.000	2.713	1.518	1.892	2.520	3.480	5.861
42.500	0.421	63.880	6.000	2.508	1.407	1.702	2.143	3.074	4.606
40.000	0.431	61.299	6.000	2.331	1.301	1.517	1.807	2.716	3.612
37.500	0.442	58.721	6.000	2.179	1.199	1.339	1.510	2.404	2.819
35.000	0.455	56.148	6.000	2.047	1.100	1.170	1.246	2.133	2.185
32.500	0.470	53.584	6.000	1.931	1.005	1.009	1.012	1.905	1.675
30.000	0.486	51.030	6.000	1.829	0.914	1.000	1.000	1.716	1.568
27.500	0.505	48.489	6.000	1.740	0.825	1.000	1.000	1.563	1.491
25.000	0.526	45.964	6.000	1.661	0.738	1.000	1.000	1.437	1.423
22.500	0.550	43.457	6.000	1.590	0.655	1.000	1.000	1.334	1.363
20.000	0.576	40.971	6.000	1.527	0.574	1.000	1.000	1.250	1.309
17.500	0.607	38.506	6.000	1.470	0.495	1.000	1.000	1.182	1.260
15.000	0.642	36.066	6.000	1.419	0.418	1.000	1.000	1.128	1.216
12.500	0.682	33.654	6.000	1.372	0.343	1.000	1.000	1.085	1.176
10.000	0.728	31.273	6.000	1.328	0.270	1.000	1.000	1.052	1.139
7.500	0.781	28.930	6.000	1.287	0.200	1.000	1.000	1.028	1.103
5.000	0.843	26.631	6.000	1.247	0.131	1.000	1.000	1.012	1.069
2.500	0.915	24.387	6.000	1.207	0.065	1.000	1.000	1.003	1.035
1.000	0.965	23.071	6.000	1.183	0.026	1.000	1.000	1.000	1.014

Table 3b. Mach Reflection for the Case of Strong Shock and Ideal Gas, $\gamma = 7/5$ (Continued)

		Region 5				Interfaces			
θ	$\bar{M}_5$	$\frac{\rho_5}{\rho_2}$	$\frac{\bar{u}_5}{u_1}$	$\frac{\tilde{u}_5}{u_1}$	$\frac{\bar{u}_1}{\bar{u}_a}$	$\frac{p_1}{p_3}$	$\frac{\bar{u}_a}{u_1}$	$\frac{\bar{u}_w}{u_1}$	$\frac{\tilde{u}_w}{u_1}$
68.231	2.697	1.844	0.398	-0.051	0.632	1.041	0.449	2.247	2.696
65.000	2.103	1.249	0.452	0.050	0.743	1.056	0.402	2.012	2.414
62.500	2.028	1.205	0.480	0.107	0.834	1.071	0.373	1.864	2.237
60.000	1.952	1.165	0.504	0.156	0.921	1.087	0.348	1.739	2.087
57.500	1.874	1.130	0.524	0.198	1.003	1.104	0.326	1.632	1.958
55.000	1.795	1.100	0.543	0.235	1.081	1.122	0.308	1.539	1.847
52.500	1.714	1.075	0.559	0.267	1.154	1.140	0.292	1.459	1.750
50.030	1.633	1.054	0.573	0.295	1.223	1.158	0.278	1.389	1.667
47.500	1.549	1.036	0.586	0.320	1.289	1.176	0.265	1.326	1.591
45.000	1.463	1.023	0.596	0.342	1.350	1.194	0.254	1.271	1.525
42.500	1.375	1.013	0.605	0.361	1.407	1.212	0.244	1.222	1.466
40.000	1.285	1.006	0.612	0.376	1.457	1.229	0.236	1.178	1.414
37.500	1.193	1.002	0.616	0.389	1.502	1.244	0.228	1.139	1.367
35.000	1.099	1.000	0.618	0.397	1.538	1.257	0.221	1.104	1.324
32.500	1.005	1.000	0.618	0.403	1.568	1.268	0.214	1.072	1.286
30.000	0.914	1.000	0.616	0.407	1.592	1.277	0.209	1.043	1.252
27.500	0.825	1.000	0.613	0.410	1.613	1.285	0.204	1.018	1.221
25.000	0.738	1.000	0.610	0.411	1.630	1.292	0.199	0.994	1.193
22.500	0.655	1.000	0.606	0.411	1.643	1.297	0.195	0.973	1.167
20.000	0.574	1.000	0.602	0.411	1.653	1.301	0.191	0.953	1.144
17.500	0.495	1.000	0.597	0.410	1.661	1.304	0.187	0.936	1.123
15.000	0.418	1.000	0.592	0.408	1.666	1.306	0.184	0.919	1.103
12.500	0.343	1.000	0.587	0.406	1.670	1.308	0.181	0.904	1.084
10.000	0.270	1.000	0.582	0.404	1.673	1.309	0.178	0.889	1.067
7.500	0.200	1.000	0.576	0.401	1.675	1.310	0.175	0.875	1.050
5.000	0.131	1.000	0.571	0.399	1.677	1.311	0.172	0.862	1.034
2.500	0.065	1.000	0.565	0.396	1.678	1.311	0.170	0.848	1.017
1.000	0.026	1.000	0.562	0.394	1.678	1.311	0.168	0.839	1.007

Table 3c. Mach Reflection for the Case of Strong Shock and Ideal Gas, $\gamma = 5/3$

		Region 1					Region 2			
θ	ω	M_1	β	$\frac{\rho_1}{\rho_0}$	$\frac{p_1}{M_1^2 p_0}$	M_2	δ	ω	$\frac{\rho_2}{\rho_1}$	$\frac{p_2}{p_1}$
64.783	0.000	3.825	6.715	4.000	1.250	2.180	18.503	15.636	2.423	5.509
62.500	0.555	3.547	7.242	4.000	1.250	2.095	18.040	16.744	2.309	4.87[illegible]
60.000	1.169	3.280	7.836	4.000	1.250	2.005	17.499	18.057	2.192	4.29[illegible]
57.500	1.792	3.045	8.446	4.000	1.250	1.918	16.922	19.478	2.085	3.831
55.000	2.425	2.835	9.075	4.000	1.250	1.834	16.309	21.011	1.985	3.44[illegible]
54.660	2.513	2.809	9.162	4.000	1.250	1.823	16.223	21.228	1.972	3.39[illegible]
52.500	3.072	2.648	9.724	4.000	1.250	1.754	15.661	22.660	1.893	3.11[illegible]
50.000	3.733	2.479	10.394	4.000	1.250	1.677	14.979	24.430	1.809	2.8[illegible]
47.500	4.412	2.326	11.086	4.000	1.250	1.604	14.262	26.327	1.732	2.612
45.000	5.111	2.186	11.802	4.000	1.250	1.535	13.514	28.357	1.661	2.412
42.500	5.832	2.059	12.544	4.000	1.250	1.470	12.733	30.526	1.596	2.23[illegible]
40.000	6.580	1.942	13.310	4.000	1.250	1.408	11.922	32.842	1.536	2.06[illegible]
37.500	7.357	1.835	14.104	4.000	1.250	1.350	11.082	35.311	1.482	1.93[illegible]
35.000	8.168	1.737	14.924	4.000	1.250	1.295	10.215	37.941	1.432	1.8[illegible]
32.500	9.017	1.646	15.770	4.000	1.250	1.245	9.324	40.738	1.387	1.7[illegible]
30.000	9.910	1.562	16.641	4.000	1.250	1.198	8.412	43.710	1.345	1.6[illegible]
27.500	10.852	1.484	17.535	4.000	1.250	1.155	7.484	46.862	1.306	1.5[illegible]
25.000	11.849	1.413	18.448	4.000	1.250	1.116	6.547	50.196	1.271	1.49[illegible]
22.500	12.910	1.348	19.375	4.000	1.250	1.081	5.610	53.712	1.238	1.4[illegible]
20.000	14.040	1.289	20.309	4.000	1.250	1.051	4.683	57.406	1.207	1.37[illegible]
17.500	15.250	1.234	21.240	4.000	1.250	1.025	3.781	61.268	1.178	1.31[illegible]
15.000	16.547	1.186	22.157	4.000	1.250	1.004	2.922	65.277	1.151	1.2[illegible]
12.500	17.941	1.142	23.046	4.000	1.250	0.989	2.127	69.406	1.125	1.21[illegible]
10.000	19.440	1.104	23.891	4.000	1.250	0.979	1.420	73.614	1.100	1.17[illegible]
7.500	21.050	1.071	24.678	4.000	1.250	0.975	0.829	77.848	1.075	1.12[illegible]
5.000	22.775	1.047	25.392	4.000	1.250	0.977	0.379	82.043	1.051	1.08[illegible]
2.500	24.616	1.019	26.022	4.000	1.250	0.986	0.097	86.121	1.026	1.04[illegible]
1.000	25.773	1.007	26.358	4.000	1.250	0.993	0.016	88.478	1.010	1.01[illegible]

Table 3c. Mach Reflection for the Case of Strong Shock and Ideal Gas, $\gamma = 5/3$ (Continued)

			Region 3			Region 4			
θ	M_3	α	$\frac{\rho_3}{\rho_0}$	$\frac{P_3}{M_1^2 P_0}$	$\bar{M}_2$	$\frac{\rho_4}{\rho_2}$	$\frac{P_4}{P_2}$	$\frac{P_{5,4}}{P_3}$	$\frac{P_4}{P_1}$
64.783	0.447	90.000	4.000	6.886	2.876	2.935	10.089	12.604	55.583
62.500	0.448	87.783	4.000	6.087	1.415	1.601	2.253	3.444	10.969
60.000	0.449	85.335	4.000	5.373	1.340	1.498	1.995	3.15[illegible]	8.577
57.500	0.451	82.868	4.000	4.789	1.267	1.394	1.756	2.878	6.727
55.000	0.454	80.384	4.000	4.305	1.195	1.290	1.534	2.63[illegible]	5.284
54.660	0.454	80.045	4.000	4.245	1.185	1.276	1.506	2.598	5.113
52.500	0.457	77.885	4.000	3.899	1.124	1.186	1.33[illegible]	2.404	4.149
50.000	0.462	75.372	4.000	3.557	1.056	1.083	1.143	2.202	3.252
47.500	0.468	72.849	4.000	3.265	0.988	1.000	1.000	2.023	2.612
45.000	0.475	70.316	4.000	3.015	0.923	1.000	1.000	1.868	2.412
42.500	0.483	67.777	4.000	2.799	0.859	1.000	1.000	1.734	2.239
40.000	0.493	65.232	4.000	2.611	0.797	1.000	1.000	1.617	2.089
37.500	0.503	62.686	4.000	2.447	0.737	1.000	1.000	1.516	1.957
35.000	0.516	60.138	4.000	2.302	0.678	1.000	1.000	1.428	1.842
32.500	0.530	57.593	4.000	2.175	0.621	1.000	1.000	1.353	1.74[illegible]
30.000	0.546	55.053	4.000	2.062	0.565	1.000	1.000	1.288	1.649
27.500	0.564	52.519	4.000	1.961	0.511	1.000	1.000	1.232	1.568
25.000	0.584	49.995	4.000	1.870	0.458	1.000	1.000	1.184	1.496
22.500	0.607	47.485	4.000	1.788	0.406	1.000	1.000	1.143	1.43[illegible]
20.000	0.633	44.992	4.000	1.713	0.356	1.000	1.000	1.109	1.371
17.500	0.662	42.521	4.000	1.645	0.307	1.000	1.000	1.080	1.316
15.000	0.695	40.079	4.000	1.582	0.259	1.000	1.000	1.057	1.265
12.500	0.732	37.673	4.000	1.522	0.213	1.000	1.000	1.038	1.218
10.000	0.774	35.312	4.000	1.466	0.168	1.000	1.000	1.024	1.172
7.500	0.821	33.007	4.000	1.411	0.124	1.000	1.000	1.013	1.129
5.000	0.874	30.771	4.000	1.357	0.081	1.000	1.000	1.006	1.086
2.500	0.934	28.619	4.000	1.304	0.040	1.000	1.000	1.001	1.043
1.000	0.973	27.374	4.000	1.272	0.016	1.000	1.000	1.000	1.017

Table 3c. Mach Reflection for the Case of Strong Shock and Ideal Gas, $\gamma = 5/3$ (Continued)

	Region 5				Interfaces				
θ	$\bar{M}_5$	$\frac{\rho_5}{\rho_2}$	$\frac{\bar{u}_5}{u_i}$	$\frac{\tilde{u}_5}{u_i}$	$\frac{\bar{u}_1}{u_{1B}}$	$\frac{p_1}{p_3}$	$\frac{u_{1B}}{u_i}$	$\frac{\bar{u}_1}{u_i}$	$\frac{\tilde{u}_1}{u_i}$
64.783	2.295	1.364	0.254	-0.333	0.279	1.013	0.587	1.760	2.347
62.500	1.385	1.017	0.302	-0.250	0.331	1.018	0.552	1.655	2.207
60.000	1.322	1.010	0.333	-0.186	0.384	1.025	0.518	1.555	2.073
57.500	1.257	1.006	0.359	-0.131	0.434	1.032	0.489	1.468	1.957
55.000	1.194	1.002	0.380	-0.084	0.480	1.039	0.464	1.392	1.856
52.500	1.141	1.001	0.383	-0.078	0.486	1.040	0.461	1.382	1.843
52.500	1.123	1.001	0.398	-0.043	0.522	1.046	0.442	1.325	1.766
50.000	1.055	1.000	0.413	-0.009	0.561	1.053	0.422	1.265	1.687
47.500	0.988	1.000	0.424	0.020	0.597	1.060	0.404	1.212	1.616
45.000	0.923	1.000	0.434	0.046	0.629	1.067	0.388	1.165	1.553
42.500	0.859	1.000	0.441	0.067	0.658	1.074	0.374	1.122	1.496
40.000	0.797	1.000	0.447	0.086	0.685	1.080	0.361	1.084	1.445
37.500	0.737	1.000	0.452	0.102	0.709	1.086	0.350	1.049	1.399
35.000	0.678	1.000	0.455	0.115	0.730	1.091	0.339	1.018	1.357
32.500	0.621	1.000	0.457	0.127	0.749	1.096	0.330	0.989	1.319
30.000	0.565	1.000	0.458	0.137	0.765	1.101	0.321	0.963	1.284
27.500	0.511	1.000	0.458	0.145	0.780	1.105	0.313	0.939	1.252
25.000	0.458	1.000	0.457	0.152	0.793	1.108	0.306	0.917	1.223
22.500	0.406	1.000	0.456	0.157	0.804	1.111	0.299	0.897	1.196
20.000	0.356	1.000	0.455	0.162	0.814	1.114	0.293	0.878	1.171
17.500	0.307	1.000	0.453	0.166	0.823	1.117	0.287	0.860	1.147
15.000	0.259	1.000	0.451	0.170	0.831	1.119	0.281	0.844	1.125
12.500	0.213	1.000	0.449	0.173	0.838	1.121	0.276	0.828	1.103
10.000	0.168	1.000	0.447	0.176	0.845	1.123	0.271	0.812	1.083
7.500	0.124	1.000	0.445	0.180	0.853	1.126	0.266	0.797	1.062
5.000	0.081	1.000	0.443	0.183	0.861	1.128	0.261	0.782	1.042
2.500	0.040	1.000	0.442	0.187	0.871	1.131	0.255	0.766	1.021
1.000	0.016	1.000	0.441	0.189	0.877	1.133	0.252	0.756	1.009

Table 4a. Variation of Pressure with Range for Height-of-Burst Case, Regular Reflection Regime

γ	$\frac{x}{h}$	ϵ	$\frac{1}{2}\left(\frac{h^3 P_1}{BE}\right)_{GB}$	$\frac{h^3 P_1}{BE}$	$\frac{h^3 P_2}{BE}$
9/7	0.000	90.000	∞	1.000	10.000
	0.087	85.000	1493.292	0.989	9.829
	0.176	80.000	182.408	0.955	9.333
	0.268	75.000	51.981	0.901	8.556
	0.364	70.000	20.740	0.830	7.568
	0.466	65.000	9.862	0.744	6.453
	0.577	60.000	5.196	0.650	5.299
	0.700	55.000	2.913	0.550	4.196
	0.839	50.000	1.693	0.450	3.238
	0.937	46.877	1.217	0.389	2.978
7/5	0.000	90.000	∞	1.000	8.000
	0.087	85.000	1493.292	0.989	7.868
	0.176	80.000	182.408	0.955	7.485
	0.268	75.000	51.981	0.901	6.885
	0.364	70.000	20.740	0.830	6.121
	0.466	65.000	9.862	0.744	5.259
	0.577	60.000	5.196	0.650	4.371
	0.700	55.000	2.913	0.550	3.539
	0.838	50.030	1.698	0.450	3.134
5/3	0.000	90.000	∞	1.000	6.000
	0.087	85.000	1493.292	0.989	5.908
	0.176	80.000	182.408	0.955	5.642
	0.268	75.000	51.981	0.901	5.225
	0.364	70.000	20.740	0.830	4.696
	0.466	65.000	9.862	0.744	4.105
	0.577	60.000	5.196	0.650	3.521
	0.700	55.000	2.913	0.550	3.194
	0.709	54.655	2.803	0.543	3.369

Table 4b. Variation of Pressure with Range for Height-of-Burst Case, Mach Reflection Regime

γ	$\frac{x}{h}$	$\frac{y_T}{h}$	θ	$\frac{1}{2}\left(\frac{h^3 p_1}{BE}\right)_{CB}$	$\frac{h^3 p_1}{BE}$	$\frac{h^3 p_3}{BE}$	$\frac{h^3 p_{s,4}}{BE}$
9/7	0.937	0.000	46.877	1.217	0.389	0.943	5.615
	0.996	0.004	45.000	1.011	0.357	0.812	4.358
	1.081	0.009	42.500	0.791	0.317	0.665	3.102
	1.173	0.016	40.000	0.620	0.279	0.542	2.199
	1.272	0.024	37.500	0.486	0.243	0.441	1.552
	1.380	0.033	35.000	0.380	0.209	0.356	1.088
	1.499	0.045	32.500	0.297	0.178	0.287	0.758
	1.630	0.059	30.000	0.231	0.150	0.229	0.525
	1.775	0.076	27.500	0.179	0.125	0.181	0.362
	1.937	0.097	25.000	0.138	0.102	0.142	0.250
	2.119	0.122	22.500	0.105	0.083	0.110	0.173
	2.325	0.154	20.000	0.080	0.066	0.084	0.120
	2.559	0.193	17.500	0.060	0.052	0.064	0.083
	2.828	0.242	15.000	0.044	0.040	0.047	0.057
	3.138	0.304	12.500	0.032	0.030	0.035	0.039
	3.498	0.383	10.000	0.023	0.022	0.025	0.027
	3.916	0.484	7.500	0.017	0.016	0.018	0.018
	4.402	0.615	5.000	0.012	0.012	0.012	0.013
	4.967	0.783	2.500	0.008	0.008	0.008	0.008
	5.346	0.907	1.000	0.007	0.007	0.007	0.007
7/5	0.838	0.000	50.030	1.698	0.450	1.250	5.584
	0.912	0.004	47.500	1.317	0.406	1.028	4.051
	0.990	0.010	45.000	1.030	0.364	0.847	2.946
	1.074	0.016	42.500	0.808	0.324	0.696	2.139
	1.163	0.024	40.000	0.635	0.286	0.571	1.550
	1.260	0.033	37.500	0.500	0.250	0.466	1.121
	1.365	0.044	35.000	0.393	0.216	0.379	0.809
	1.479	0.058	32.500	0.309	0.185	0.307	0.585
	1.604	0.074	30.000	0.242	0.157	0.247	0.424
	1.742	0.093	27.500	0.189	0.132	0.197	0.308
	1.894	0.117	25.000	0.147	0.110	[illegible]	[illegible]
	2.063	0.145	22.500	0.114	0.090	[illegible]	0.16[illegible]
	2.252	0.180	20.000	0.088	0.073	[illegible]095	0.11[illegible]
	2.465	0.223	17.500	0.067	0.058	0.073	0.086
	2.704	0.275	15.000	0.051	0.046	0.055	0.063
	2.975	0.340	12.500	0.038	0.035	0.042	0.045
	3.283	0.421	10.000	0.028	0.027	0.031	0.032
	3.632	0.522	7.500	0.021	0.020	0.022	0.023
	4.028	0.648	5.000	0.015	0.015	0.016	0.016
	4.476	0.805	2.500	0.011	0.011	0.012	0.012
	4.772	0.917	1.000	0.009	0.009	0.009	0.009
5/3	0.709	0.000	54.655	2.803	0.543	1.843	4.788
	0.765	0.003	52.500	2.232	0.503	1.571	3.776
	0.833	0.007	50.000	1.728	0.459	1.306	2.875
	0.905	0.012	47.500	1.347	0.415	1.085	2.196
	0.982	0.018	45.000	1.057	0.374	0.901	1.684
	1.063	0.026	42.500	0.833	0.334	0.747	1.296
	1.149	0.035	40.000	0.658	0.296	0.618	1.000
	1.242	0.047	37.500	0.522	0.261	0.510	0.773
	1.342	0.060	35.000	0.414	0.227	0.419	0.599
	1.449	0.077	32.500	0.328	0.197	0.343	0.464
	1.566	0.096	30.000	0.261	0.169	0.279	0.359
	1.692	0.119	27.500	0.206	0.144	0.226	0.278
	1.830	0.147	25.000	0.163	0.122	0.182	0.215
	1.980	0.180	22.500	0.129	0.102	0.145	0.166
	2.145	0.219	20.000	0.101	0.084	0.115	0.128
	2.326	0.267	17.500	0.080	0.069	0.091	0.098
	2.525	0.323	15.000	0.062	0.056	0.071	0.075
	2.744	0.392	12.500	0.048	0.045	0.055	0.057
	2.986	0.473	10.000	0.038	0.036	0.042	0.043
	3.252	0.572	7.500	0.029	0.028	0.032	0.032
	3.545	0.690	5.000	0.022	0.022	0.024	0.024
	3.867	0.831	2.500	0.017	0.017	0.018	0.018
	4.075	0.929	1.000	0.015	0.015	0.015	0.015

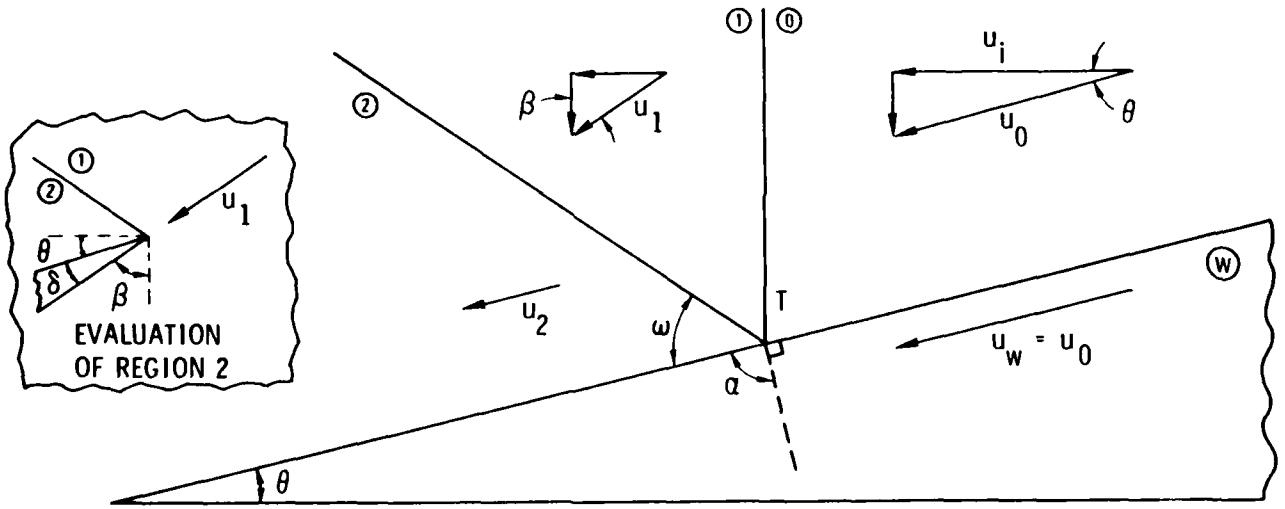

Fig. 5. Regular Reflection, Point T Stationary

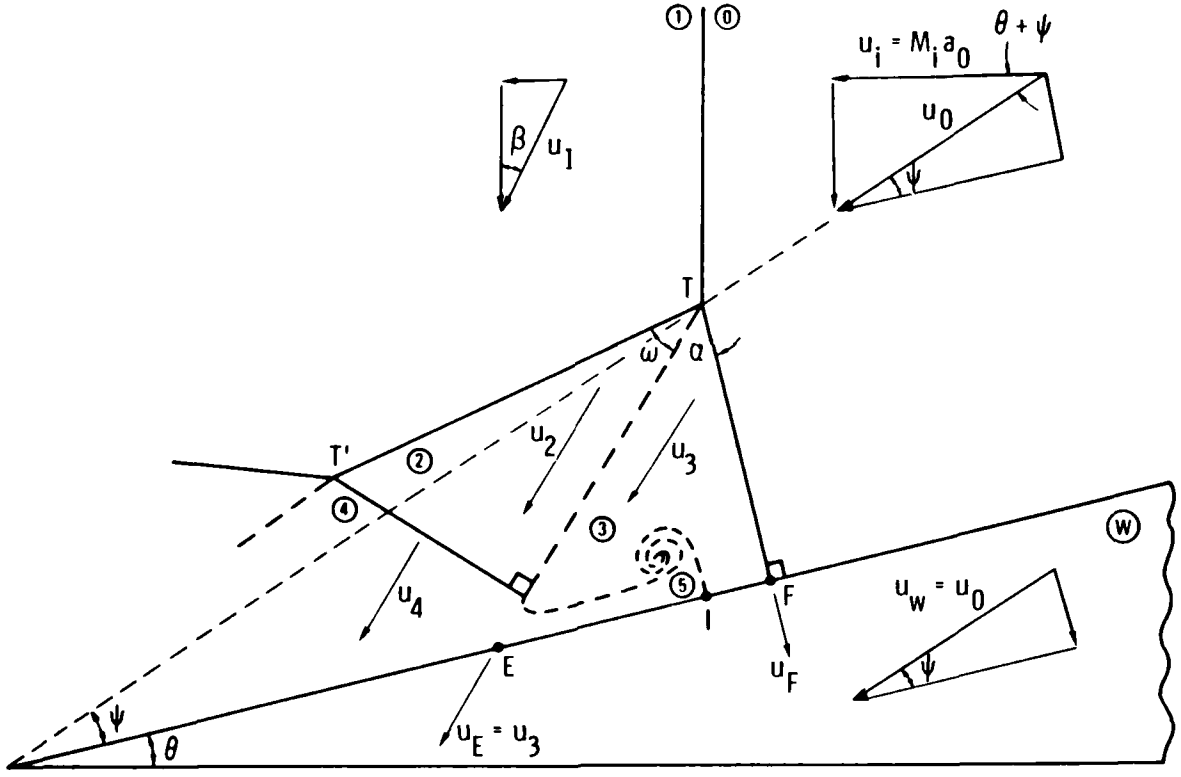

Fig. 6a. Mach Reflection Flow Field in Various Coordinate Systems, Point T Stationary

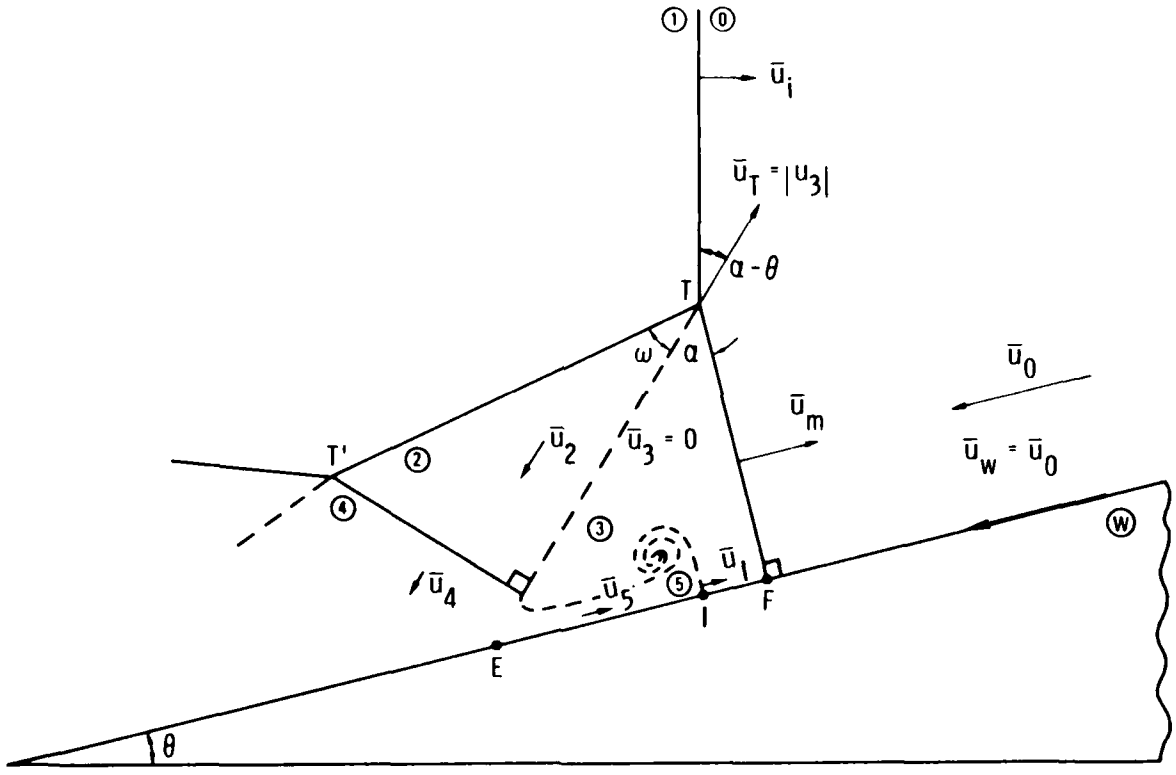

Fig. 6b. Mach Reflection Flow Field in Various Coordinate Systems, Point E Stationary

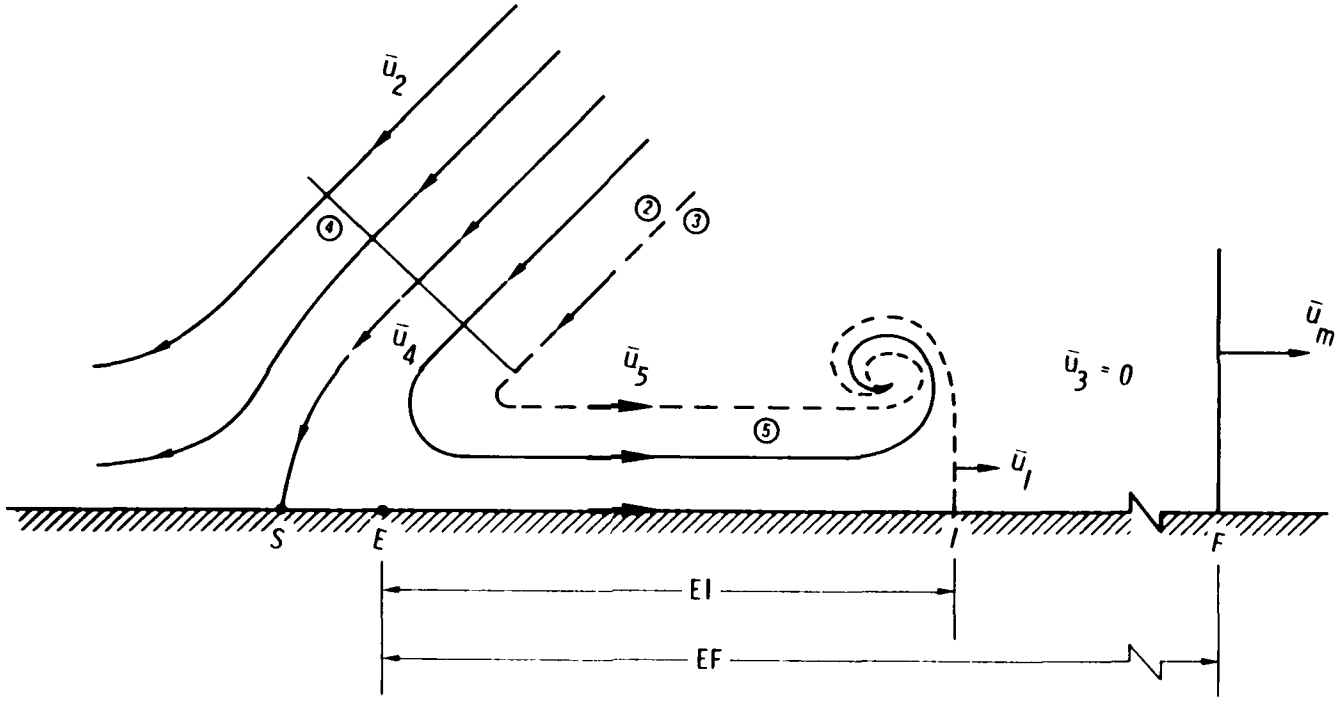

Fig. 6c. Mach Reflection Flow Field in Various Coordinate Systems, Point E Stationary (exploded view)

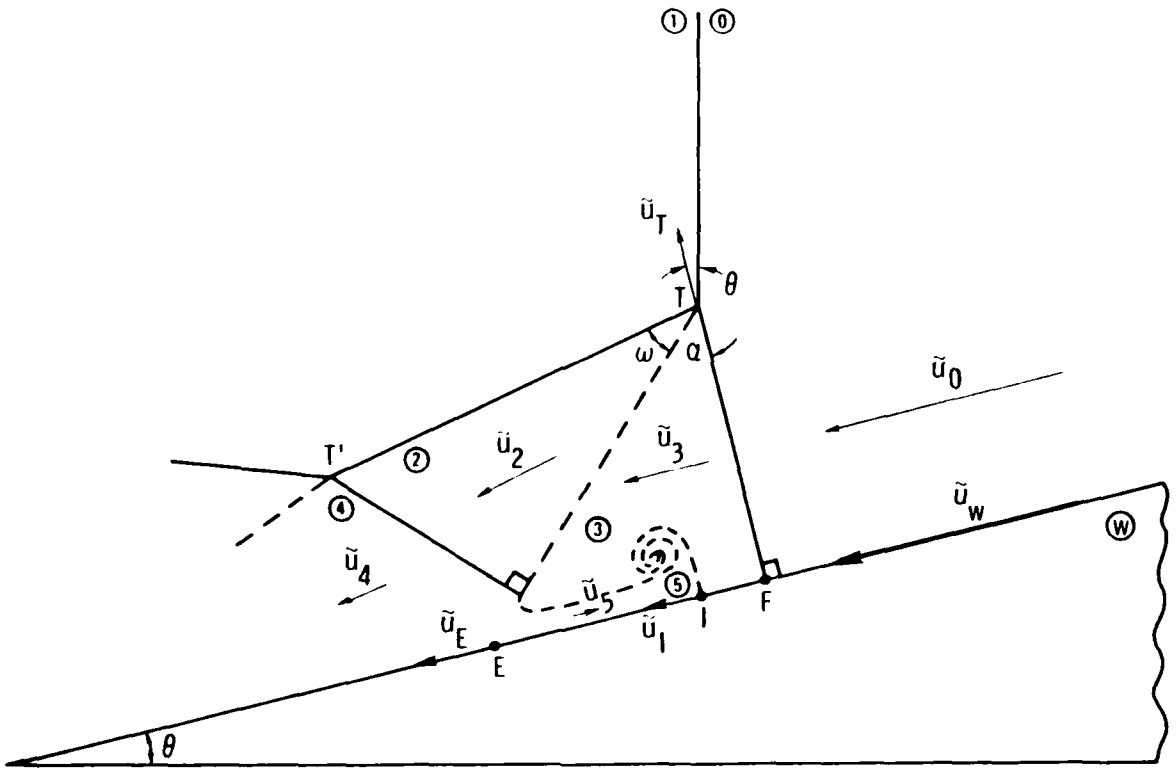

Fig. 6d. Mach Reflection Flow Field in Various Coordinate Systems, Point F Stationary

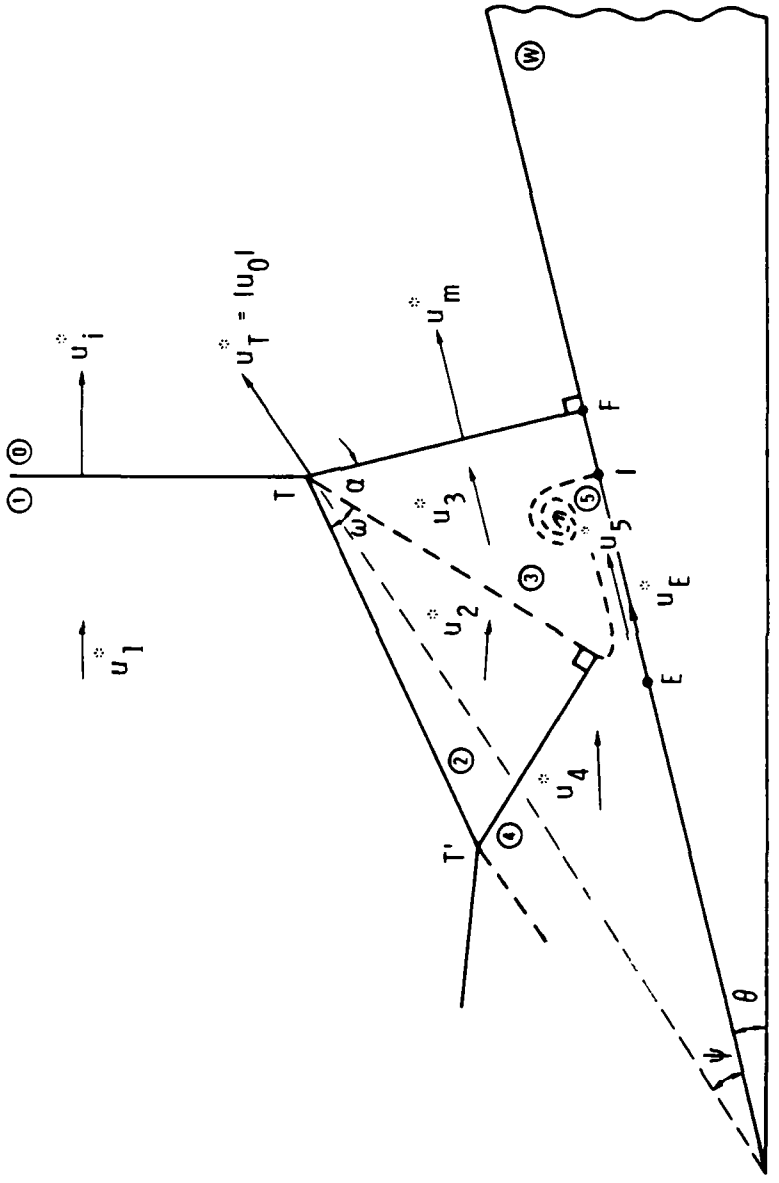

Fig. 6e. Mach Reflection Flow Field in Various Coordinate Systems, Wall Stationary

B. MACH REFLECTION

Mach reflection flow-field properties are deduced in Appendix B. The triple-point region (regions 1, 2, and 3), the criteria for the transition from double (DMR) to complex (CRM) to simple (SMR) Mach reflections, and the recirculation region (regions 4 and 5) are discussed herein.

1. REGIONS 1, 2, AND 3

The flow in regions 1, 2, and 3 is a classical triple-point flow and is obtained subject to the assumptions that $p_2 = p_3$ and that the primary Mach stem (denoted m in Fig. 4) is perpendicular to the wedge. Numerical results for regions 1, 2, and 3 are presented in Table 3 for values of θ in the range $\theta > \theta_D$ (for which either a regular or a Mach reflection can exist) and for values of θ in the range $\theta < \theta_D$ (for which only a Mach reflection can exist). The range $\theta < \theta_D$ is of primary interest since it is generally assumed that the transition from regular to Mach reflection occurs at θ_D for wedge and HOB flows.

It is seen in Table 3 that $M_2 > \bar{M} > 1$ at $\theta = \theta_D$. The quantities M_2 and $\bar{M}_2$ denote the Mach number in region 2 relative to points T and E, respectively (e.g., Figs. 6a and 6b). Both M_2 and $\bar{M}_2$ decrease as θ decreases. The values of θ at which $\bar{M}_2 = 1$ and at which $M_2 = 1$ are noted in Table 2. The transition from double- to complex- to simple-Mach reflection can be explained in terms of the variation of M_2 and $\bar{M}_2$ with decrease in θ, from θ_D, as is discussed in the next section.

2. TRANSITION CRITERIA

The second Mach stem m′ (Fig. 4) is expected to occur near point E when $\bar{M}_2 > 1$. Hence for values of θ near θ_D, a double-Mach reflection occurs with flows similar to those depicted in Fig. 6. The location of the second Mach stem, near point E, is expected to persist, with decrease in θ until a value of θ is reached at which $\bar{M}_2 = 1$. The value of θ corresponding to $\bar{M}_2 = 1$ is termed θ_{DMR1} herein and is listed in Table 2 for several values of γ. The angle θ_{DMR1} is the lowest wedge angle at which the second Mach stem remains near point E. With further decrease in θ, $\bar{M}_2$ becomes subsonic while M_2

remains supersonic, and the second Mach stem moves toward point T. At some value of θ, termed θ_{CMR}, the second Mach stem is no longer apparent in interferograms and the transition to complex-Mach reflection is said to occur. References 2 and 3 have proposed that the transition angle θ_{CMR} corresponds approximately to the Mach number condition $M_2 = 1.3$. Although this criterion is not well established, it has been used to determine the values of θ_{CMR} listed in Table 2. With further decrease in θ, a value, termed θ_{SMR}, is reached at which $M_2 = 1$. The transition from CMR to SMR occurs at θ_{SMR} (see Table 2). The present results for critical angles agree with the results of Refs. 2 and 3 (for $\gamma = 7/5, 5/3$) and Ref. 4 (for $\gamma = 9/7$) in the limit of large values of M_1, except for the value of θ_{CMR} in Ref. 4. The latter value appears to correspond to $M_2 = 1.2$ rather than $M_2 = 1.3$, as noted in Fig. 2 and Table 2. All the transition criteria other than θ_{CMR} are well established. The choice for θ_{CMR} probably requires further study.

3. REGIONS 4 AND 5

Regions 4 and 5 are illustrated in Fig. 6c. Region 4 is the region downstream of the second Mach stem and region 5 is the recirculation region that results from the overpressure at stagnation point S. The evaluation of both the stagnation pressure $p_{s,4}$ and the characteristic velocity in region 5 (namely $\bar{u}_5$ in Fig. 6c) is a major objective of the present study. These quantities are evaluated in Appendix B by considering two regimes, namely $\bar{M}_2 > 1$ and $\bar{M}_2 < 1$. When $\bar{M}_2 > 1$ it is assumed that the second Mach stem is at point E and conditions in regions 2 and 4 are related by a shock of strength $\bar{M}_2$. When $\bar{M}_2 < 1$, it is assumed that the second shock stem, if it exists, is sufficiently weak that the pressure $p_{s,4}$ is isentropically related to conditions in region 2. In both cases ($\bar{M}_2 > 1$ and $\bar{M}_2 < 1$), the flow velocity in region 5 is found from an isentropic expansion from $p_{s,4}$ to the pressure $p_5 = p_2 = p_3$. Numerical results for $p_{s,4}$ and $\bar{u}_5$ are included in Table 3.

An estimate for the interface velocity $\bar{u}_I$ (Fig. 6c) is also obtained in Appendix B. The interface location

$$\frac{EI}{EF} = \frac{\bar{u}_I}{\bar{u}_m} \tag{1}$$

is included in Table 3 and is plotted in Fig. 7. The present solution is self-consistent provided $\bar{u}_I/\bar{u}_m < 1$, since the primary shock has been assumed, in Appendix B, to be unperturbed by region 5. The latter assumption is satisfied for $\gamma = 5/3$ but is violated for $\gamma = 7/5$ and 9/7. In the latter cases the recirculation region is expected to extend to the nominal primary Mach stem position and to accelerate and distort the Mach stem. Values of $\bar{u}_1/\bar{u}_M > 1$ are included in Table 3 to indicate the severity of the interaction between the recirculation region and the primary Mach stem. The interaction is seen to be more severe, with decrease in γ, as is observed experimentally.[4] An improved solution, for interface I location, is needed for those cases where the present theory indicates $\bar{u}_I/\bar{u}_M > 1$.

The point I, in Fig. 6c, is a local stagnation point in a coordinate system wherein point I is stationary. Estimates for the pressure at point I, namely p_I, are included in Table 3. (Values of p_I, corresponding to cases where $\bar{u}_I/\bar{u}_M > 1$, should be viewed as approximate.) It follows that the Mach reflection flow-field has two local surface-pressure maxima (p_I and $p_{s,4}$). These local maxima are consistent with experimental density contours (Ref. 4).

C. HEIGHT OF BURST

Height-of-burst flow fields are deduced in Appendix D and numerical results are listed in Table 4.

With increase in ground range, the HOB shock reflection process undergoes a transition from regular to Mach reflection. Solutions for triple-point trajectory and for surface pressure behind the incident shock are deduced, in Appendix D, by assuming that the rate of growth of the Mach reflection flow fields at each instant is the same as that for a corresponding wedge flow. The resulting solutions are then functions only of ground range (x/h) and γ. Triple-point coordinates x/h, y_T/h are listed in Table 4b and plotted in Fig. 8. Surface pressures, in the form h^3p/BE, are included in Table 4 and are plotted in Fig. 9. The shaded region in Fig. 8 indicates the pressure range

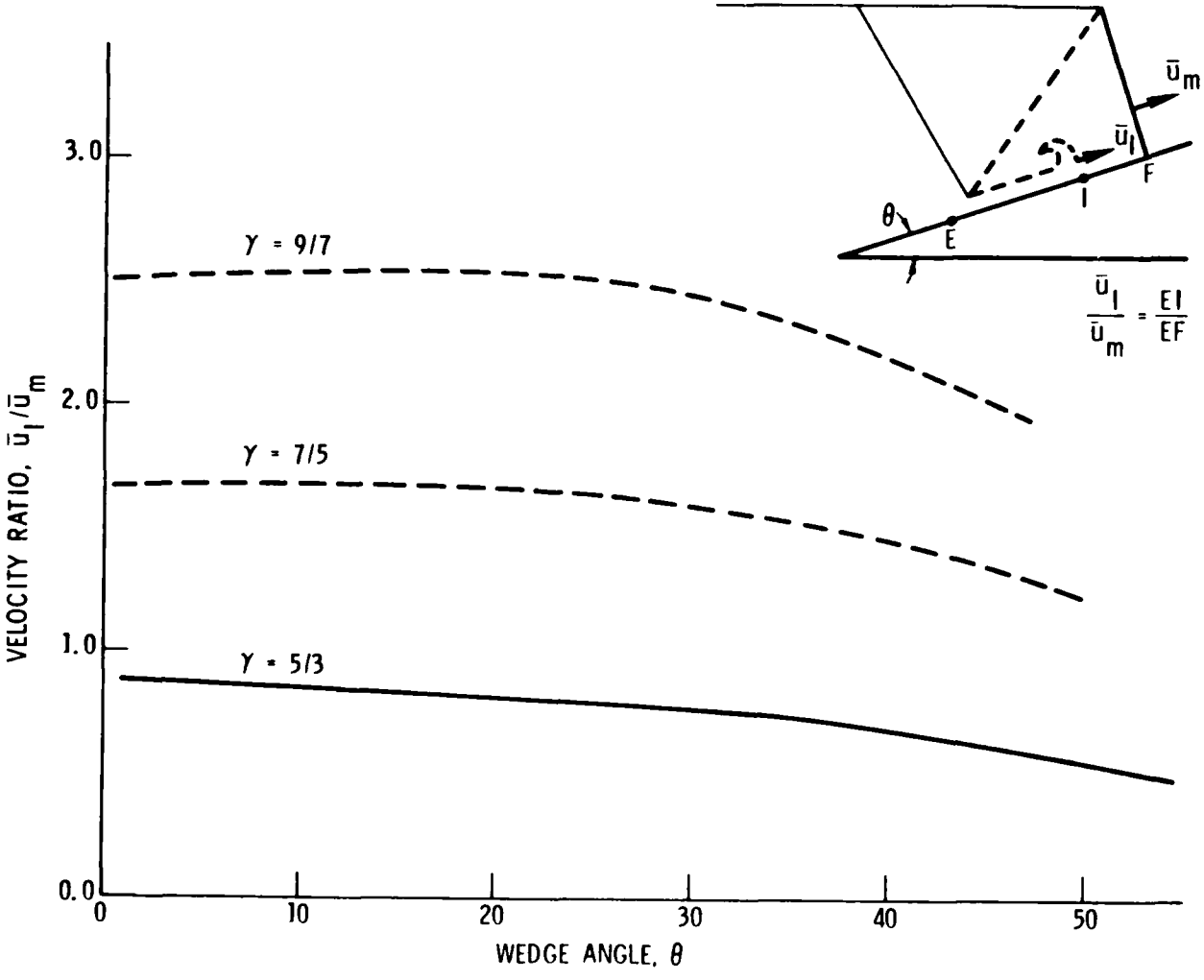

Fig. 7. Interface Velocity Ratio in Point E Stationary Coordinates. Solution invalid for $(\bar{u}_I/\bar{u}_m) > 1$.

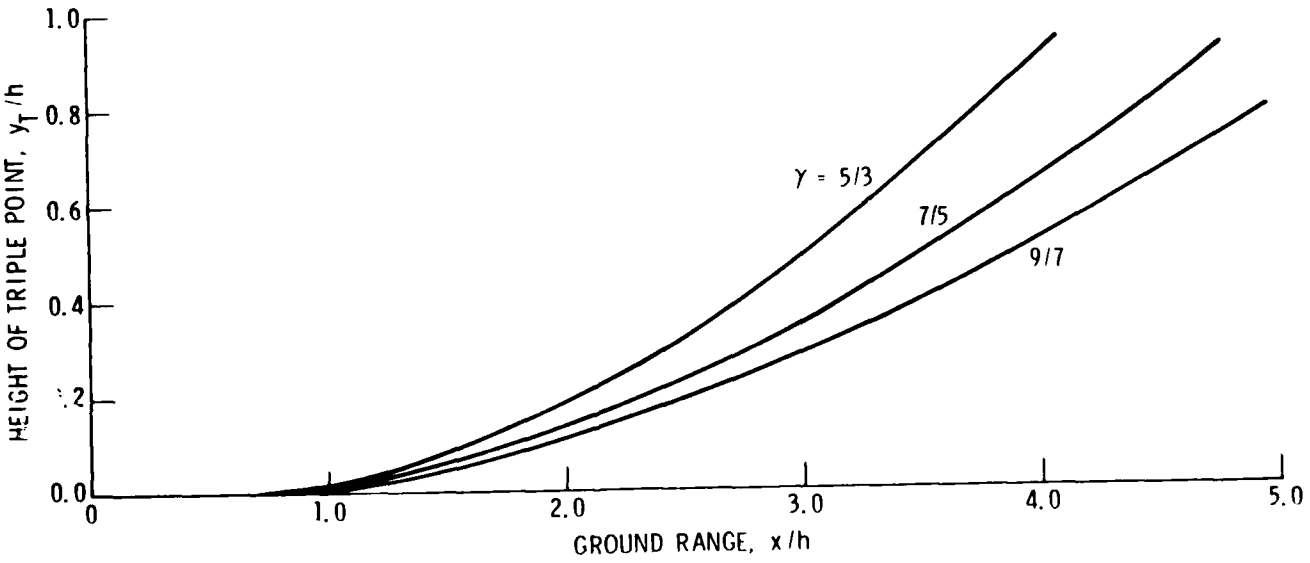

Fig. 8. Triple-Point Trajectory for Height-of-Burst Case

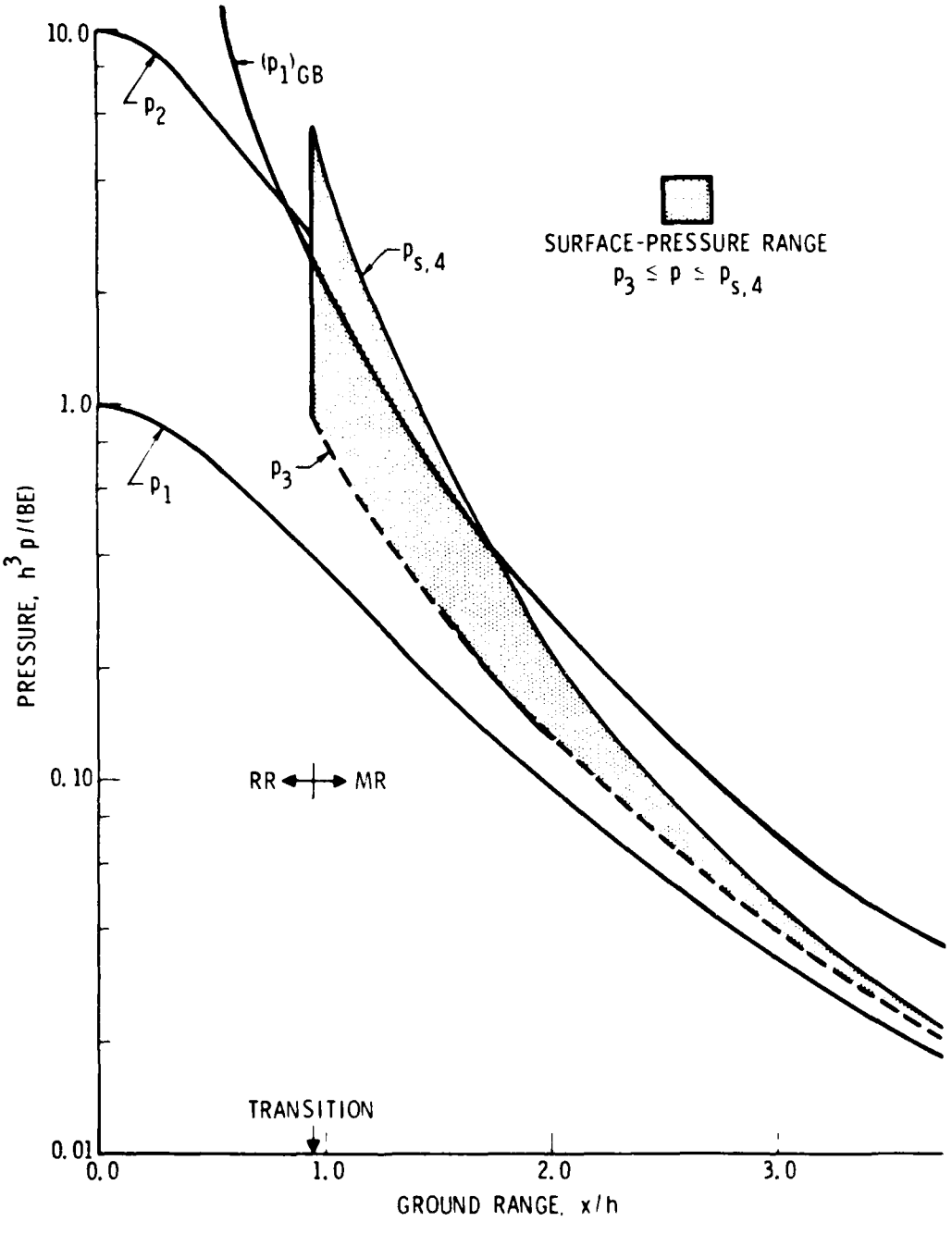

Fig. 9a. Pressures Induced by Blast Wave, $\gamma = 9/7$

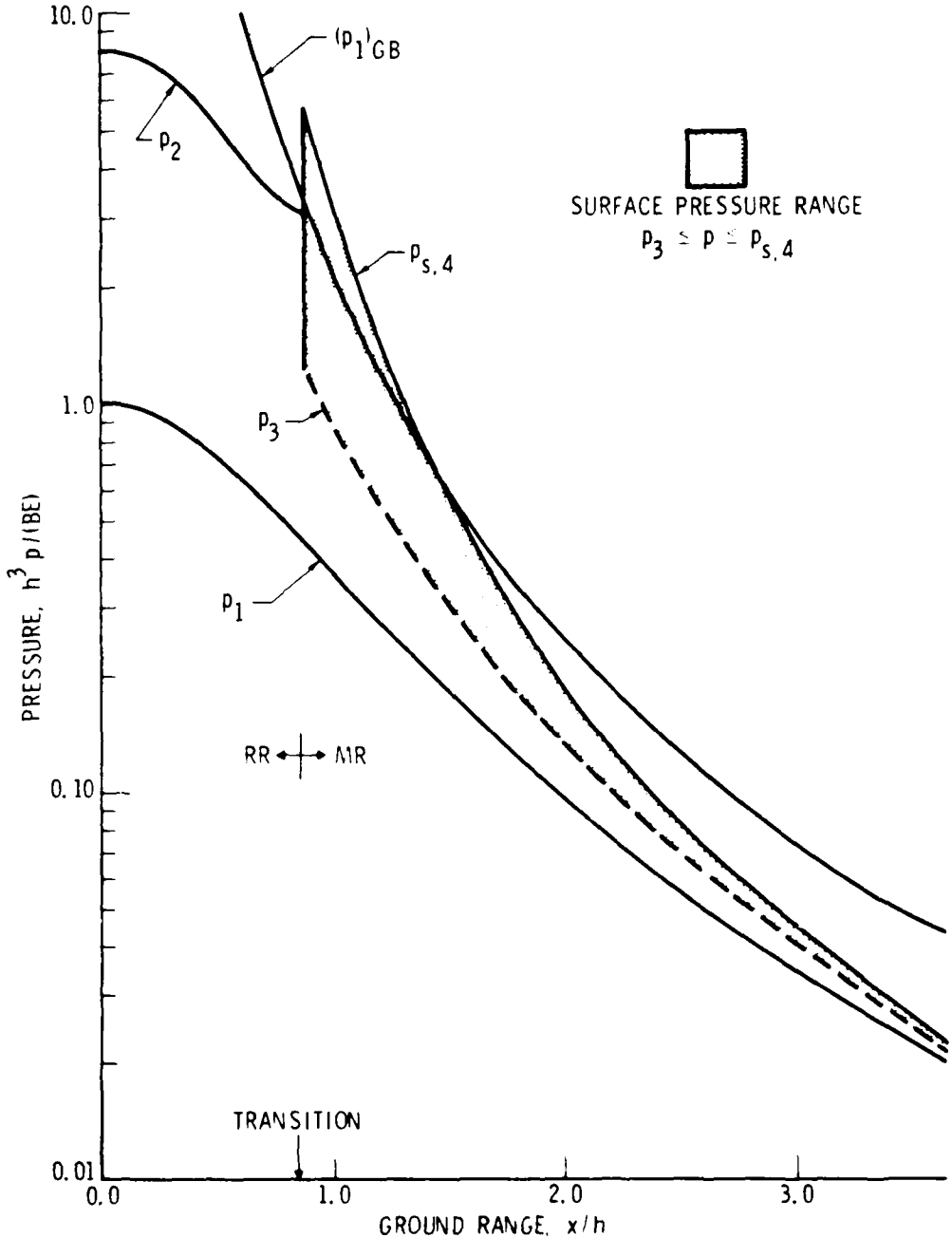

Fig. 9b. Pressures Induced by Blast Wave, $\gamma = 7/5$

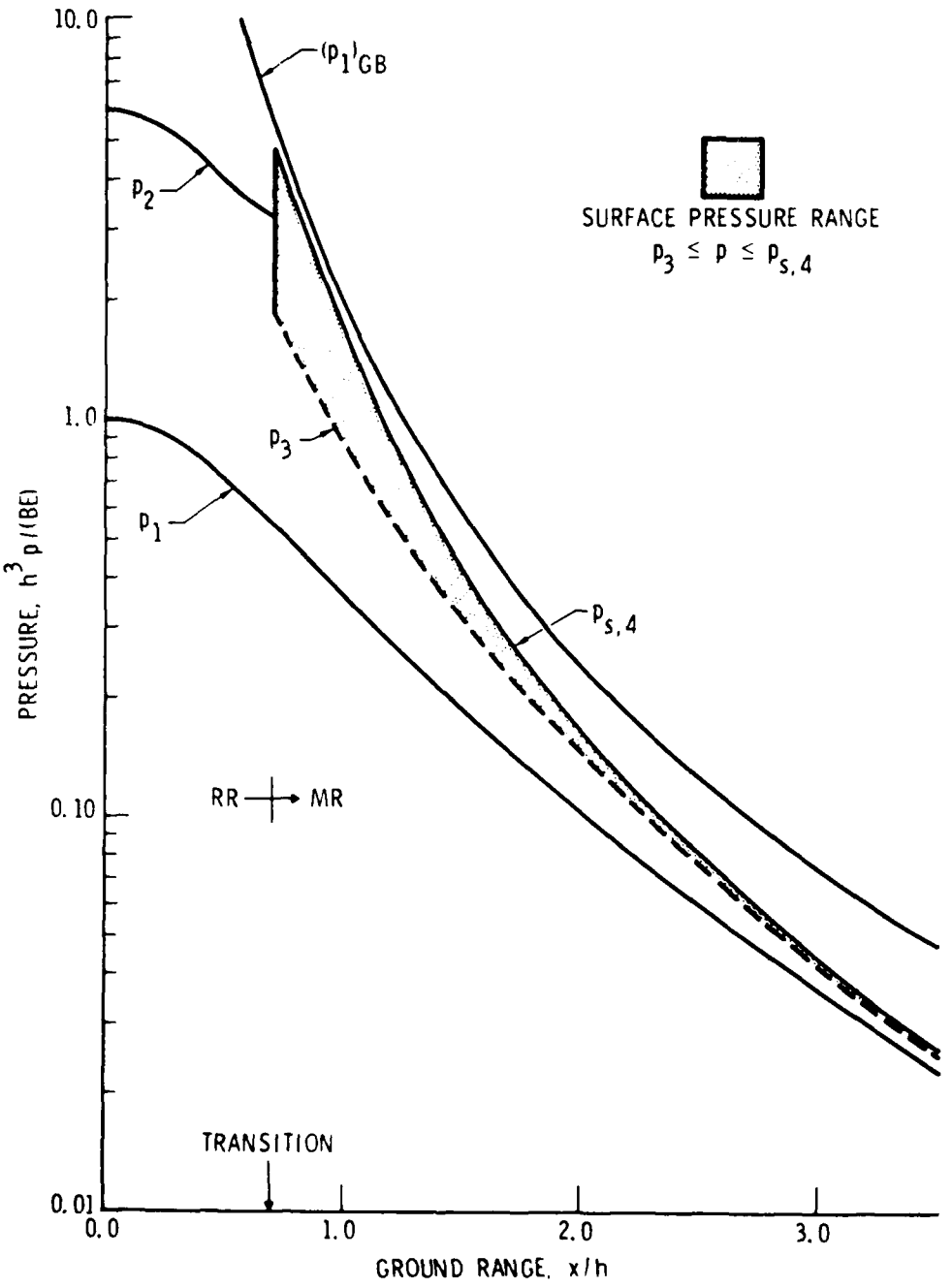

Fig. 9c. Pressures Induced by Blast Wave, $\gamma = 5/3$

$p_3 \leq p \leq p_{s,4}$, which is the range of surface pressure between points F and S in Fig. 6. Recall that there is also a local pressure maximum at point I which is only slightly larger than p_3.

The surface pressure directly behind the incident shock for the case of a ground burst (h = 0) is denoted by $(p_1)_{GB}$ and is included in Fig. 9 and Table 4. The ground burst has an effective energy of 2E. The Mach reflection process, for the HOB case, yields a peak surface pressure $p_{s,4}$ which is greater than $(p_1)_{GB}$ in only a limited ground-range region. The extent of the region for which $p_{s,4} > (p_1)_{GB}$ decreases with increase in γ. This region has the extent $0.85 < x/h < 1.80$ for $\gamma = 9/7$ and $0.84 < x/h < 1.41$ for $\gamma = 7/5$ and is nonexistent for $\gamma = 5/3$.

The present local similarity solution neglects the effect of the non-uniformity of the flow field behind the incident shock [e.g., Eqs. (D-1d) to (D-1f)]. This effect is negligible when the Mach reflection region is small compared to the shock radius R, but may become significant with an increase in x/h beyond the transition point.

III. CONCLUDING REMARKS

The present wedge model assumes an ideal gas and $M_1^2 \gg 1$ and appears to give accurate results for $M_1 \gtrsim 5$ (e.g., Fig. 2). The Mach reflection flow field associated with passage of a shock over a wedge is a function only of γ in the present limit. Numerical results have been obtained for $\gamma = 6/5$, 9/7, 7/5, and 5/3.

The present solution for the HOB flow fields provides triple-point trajectory and surface-pressure results that also depend only on γ. However, the quasisteady approximation used to obtain these results requires validation.

REFERENCES

1. T. V. Bazhenova, V. P. Fokeev, and L. G. Gvozdeva, "Regions of Various Forms of Mach Reflection and Its Transition to Regular Reflection," Acta Astronautica 3, 131 (1976).

2. G. Ben-Dor and I. I. Glass, "Domains and Boundaries of Non-Stationary Oblique Shock-Wave Reflexions. 1. Diatomic Gas," J. Fluid Mech. 92, 459 (1979).

3. G. Ben-Dor and I. I. Glass, "Domains and Boundaries of Non-Stationary Oblique Shock-Wave Reflexions. 2. Monatomic Gas," J. Fluid Mech. 96, 735 (1980).

4. S. Ando and I. I. Glass, "Domains and Boundaries of Pseudostationary Oblique Shock-Wave Reflections in Carbon Dioxide," Seventh International Symposium on Military Applications of Blast Simulation, Medicine Hat, Canada, 13-17 July 1981.

5. M. Fry, J. M. Picone, J. P. Boris, and D. L. Book, "Transition to Double-Mach Stem for Nuclear Explosion at 104-ft Height of Burst," NRL Memorandum Report 4630, 17 November 1981.

6. Ames Research Staff, "Equations, Tables, and Charts for Compressible Flow," Report 1135, 1953.

7. L. I. Sedov, "Similarity and Dimensional Methods in Mechanics," Academic Press, 1959, 210-233.

8. H. L. Brode, "Review of Nuclear Weapons Effects," Annual Review of Nuclear Science, Vol. 18 (1968), pp. 153-202.

APPENDIX A. STRONG SHOCK RELATIONS

Let subscripts 1 and 2 denote (in the present section only) conditions upstream and downstream of a shock, and let subscripts n and t denote normal and transverse velocity components, respectively. Consider the case of an ideal gas with a large Mach number component normal to the shock, $M_n^{-2} \equiv (u_{n,1}/a_1)^{-2} \ll 1$. Conditions across the shock are then (e.g., Ref. 6)

$$\frac{\rho_2}{\rho_1} = \frac{u_{n,1}}{u_{n,2}} = K_1 \left[1 + 0\left(\frac{M_n^{-2}}{\gamma - 1}\right)\right] \tag{A-1a}$$

$$\frac{u_{t,1}}{u_{t,2}} = 1 \tag{A-1b}$$

$$\frac{1}{M_n^2}\,\frac{p_2}{p_1} = K_2 \left[1 + 0\left(\frac{M_n^{-2}}{(\gamma - 1)^{-1}}\right)\right]$$

$$\frac{1}{M_n^2}\,\frac{T_2}{T_1} = \frac{1}{M_n^2}\left(\frac{a_2}{a_1}\right)^2 \tag{A-1c}$$

$$= \frac{K_2}{K_1}\left[1 + 0\left(\frac{M_n^{-2}}{\gamma - 1}\right) + 0\left(\frac{M_n^{-2}}{(\gamma - 1)^{-1}}\right)\right. \tag{A-1d}$$

where

$$K_1 = (\gamma + 1)/(\gamma - 1) \tag{A-2a}$$

$$K_2 = 2\gamma/(\gamma + 1) \tag{A-2b}$$

APPENDIX B. MACH REFLECTION

The Mach reflection associated with the passage of a planar shock wave over a wedge is considered herein for the case of a strong incident shock and an ideal gas. The flow is considered in coordinate systems wherein the points T, E, and F, respectively, (Fig. 6) are stationary. Finally, the wall stationary case is discussed.

A. POINT T STATIONARY

The flow in regions 0, 1, 2, and 3 are steady-state flows in the coordinate system wherein the triple-point T is stationary (Fig. 6a). Flow velocity and Mach number are denoted u and M, respectively. Dependent variables are found by the simultaneous solutions of equations relating the flow in regions 0 through 3. The fluid in region 0 and the wall have the same velocity, namely

$$\frac{u_0}{u_1} \equiv \frac{u_w}{u_i} = \frac{1}{\cos(\theta + \psi)} \tag{B-1}$$

Other quantities of interest are found as follows:

1. REGION 1

Strong shock relations (Appendix A) indicate

$$\cot\beta = K_1 \tan(\theta + \psi) \tag{B-2a}$$

$$\frac{u_1}{u_i} = \left(\frac{K_2}{K_1}\right)^{1/2} M_1 = \frac{1}{K_1 \sin\beta} \tag{B-2b}$$

$$\frac{1}{K_2 M_i^2} \frac{p_i}{p_0} = \frac{K_1}{K_2 M_i^2} \frac{T_1}{T_0} = \frac{1}{K_1} \frac{\rho_1}{\rho_0} = 1 \tag{B-2c}$$

2. REGION 3

Again, from strong shock relations, $\rho_3/\rho_0 = K_1$ and

$$\tan\alpha = (\cot\psi)/K_1 \tag{B-3a}$$

$$M_3 = [(1 + K_1^2 \tan^2\psi)/(K_1 K_2)]^{1/2} \tag{B-3b}$$

$$\frac{1}{K^2 M_i^2} \frac{p_3}{p_0} = \frac{K_1}{K_2 M_i^2} \frac{T_3}{T_0} = \left[\frac{\cos\psi}{\cos(\theta + \psi)}\right]^2 \tag{B-3c}$$

$$\frac{u_3}{u_i} = \left(\frac{1}{M_i^2} \frac{T_3}{T_0}\right)^{1/2} M_3 \tag{B-3d}$$

3. REGION 2

The flow in Region 2 corresponds to supersonic flow of Mach number M_1 over a wedge of half angle δ defined by

$$\delta \equiv \alpha - \theta - \beta \tag{B-4a}$$

Recall that $p_3 = p_2$ across the contact surface. It follows that

$$\xi \equiv \frac{p_2}{p_1} = \left(\frac{\cos\psi}{\cos(\theta + \psi)}\right)^2 \tag{B-4b}$$

Oblique shock relations (e.g., Ref. 6) then indicate

$$\tan^2\delta = \left(\frac{K_1K_2M_1^2}{1 + K_1\xi} - 1\right)\left(\frac{\xi - 1}{\gamma M_1^2 - \xi + 1}\right)^2 \qquad \text{(B-4c)}$$

$$M_2^2 = \frac{M_1^2\,(K_1\xi + 1) - [2/(\gamma - 1)]\,(\xi^2 - 1)}{\xi(\xi + K_1)} \qquad \text{(B-4d)}$$

$$\frac{T_2}{T_1} = \frac{\rho_1}{\rho_2}\,\xi = \frac{\xi(\xi + K_1)}{K_1\xi + 1} \qquad \text{(B-4e)}$$

$$\frac{u_2}{u_i} = \frac{M_2}{M_1}\left(\frac{T_2}{T_1}\right)^{1/2}\frac{u_1}{u_i} \qquad \text{(B-4f)}$$

$$\omega = \left[\sin^{-1}\left(\frac{\xi + K_1}{K_1K_2\xi M_2^2}\right)\right]^{1/2} \qquad \text{(B-4g)}$$

Equations (B-4c) through (B-4f) correspond to the "weak" branch of the oblique shock solution. This may be confirmed by noting that $\xi \to 1$ as $\delta \to 0$ in Eq. (B-4c). The weak solution is the one that generally occurs in physical flows.

4. SOLUTION

Equations (B-2a), (B-2b), (B-3a), (B-4a), (B-4b), and (B-4c) provide six equations for the six dependent variables ψ, β, M_1, α, δ, ξ. These equations define the flow in regions 0 through 3 and can be solved by trial and error after an initial estimate is made for ψ. Numerical results for dependent variables of interest are given in Table 1. The solution for region 4 is presented in the next section.

B. POINT E STATIONARY

Point E is defined as the intersection between the contact surface (assumed uncurled) and the wall surface. When the flow in region 2 is

supersonic, relative to E, a second Mach stem is generated (i.e., m′ in Fig. 4) that nominally originates at point E. The flow in region 4 is steady when viewed in a coordinate system wherein point E is stationary. This coordinate system is illustrated in Figs. 6b and 6c. The flow depicted therein is now evaluated.

Flow velocity and Mach number in the point E stationary coordinate system are denoted by $\bar{u}$ and $\bar{M}$, respectively, and are obtained by subtracting the vector velocity $u_E = u_3$ in Fig. 6a from the velocities shown therein. Note that $\bar{u}_3 = 0$. The free-stream, wall, and triple-point velocities are

$$\frac{\bar{u}_0}{u_i} \equiv \frac{\bar{u}_w}{u_i} = \frac{K_1 - 1}{K_1} \quad \frac{\cos\psi}{\cos(\theta + \psi)} \tag{B-5a}$$

$$\frac{\bar{u}_T}{u_i} \equiv \frac{1}{\cos(\alpha - \theta)} \quad \frac{\bar{u}_i}{u_i} = \frac{1}{\sin\alpha} \quad \frac{\bar{u}_m}{u_i} = \frac{u_3}{u_i} \tag{B-5b}$$

The flow is region 2 is

$$\frac{\bar{u}_2}{u_i} = \frac{u_2}{u_i} - \frac{u_3}{u_i} \tag{B-6a}$$

$$\bar{M}_2 = \left(M_i^2 \frac{T_0}{T_1} \quad \frac{T_1}{T_2}\right)^{1/2} \quad \frac{\bar{u}_2}{u_i} \tag{B-6b}$$

When $\bar{M}_2 > 1$, the second Mach stem m′ (Fig. 4) may be assumed to originate in the vicinity of point E. Conditions in region 4 are then found from steady-state shock relations, namely

$$\frac{p_4}{p_2} = \frac{2\gamma(\bar{M}_2)^2 - (\gamma - 1)}{\gamma + 1} \tag{B-7a}$$

$$\frac{\bar{u}_2}{\bar{u}_4} = \frac{\rho_4}{\rho_2} = \frac{p_4}{p_2}\,\frac{T_2}{T_4} = \frac{(\gamma + 1)(\bar{M}_2)^2}{(\gamma - 1)(\bar{M}_2)^2 + 2} \tag{B-7b}$$

$$\bar{M}_4 = \left[\frac{(\gamma - 1)\,(\bar{M}_2)^2 + 2}{2\gamma\,(\bar{M}_2)^2 - (\gamma - 1)}\right]^{1/2} \tag{B-7c}$$

$$\frac{p_{s,4}}{p_3} = \frac{p_{s,4}}{p_2} = \left[\frac{\gamma + 1}{2}\,(\bar{M}_2)^2\right]^{\gamma/(\gamma - 1)} \left(\frac{p_2}{p_4}\right)^{1/(\gamma - 1)} \tag{B-7d}$$

where $p_{s,4}$ is the pressure at the stagnation point S which develops in region 4 (Fig. 6c). When $\bar{M}_2 < 1$, the second Mach stem is assumed to be sufficiently weak so that the stagnation pressure at S is found from the isentropic relations*

$$\frac{p_{s,4}}{p_3} = \frac{p_{s,4}}{p_2} = \left[1 + \frac{\gamma - 1}{2}\,(\bar{M}_2)^2\right]^{\gamma/(\gamma - 1)} \tag{B-7e}$$

Equations (B-7d) and (B-7e) provide estimates of the maximum wall-surface pressure induced by the Mach reflection process and apply independently of the coordinate system. Since p_4 is larger than p_3, there will be an expansion of the flow from region 4 into region 3, as illustrated in Fig. 6c. The expanded flow is denoted region 5. The flow properties in region 5, corresponding to an isentropic expansion from region 4 to the pressure $p_5 = p_3 = p_2$, are (for $\bar{M}_2 > 1$)

$$(\bar{M}_5)^2 = \frac{2}{\gamma - 1}\left\{\left[1 + \frac{\gamma - 1}{2}\,(\bar{M}_4)^2\right]\left(\frac{p_4}{p_2}\right)^{(\gamma - 1)/\gamma} - 1\right\} \tag{B-8a}$$

$$\frac{T_5}{T_2} = \frac{\rho_2}{\rho_5} = \frac{1 + [(\gamma - 1)/2](\bar{M}_5)^2}{1 + [(\gamma - 1)/2](\bar{M}_2)^2} \tag{B-8b}$$

*See body of report for further discussion.

$$\frac{\bar{u}_5}{u_i} = \frac{\bar{M}_5}{\bar{M}_2} \frac{\bar{u}_2}{u_i} \left(\frac{T_5}{T_2}\right)^{1/2} \tag{B-8c}$$

When $\bar{M}_2 < 1$, re-expansion from the stagnation zone results in conditions in region 5 that are identical to those in region 2, except for the direction of flow. Thus, for $\bar{M}_2 < 1$

$$\frac{\bar{u}_5}{\bar{u}_2} = \frac{\bar{M}_5}{\bar{M}_2} = \frac{T_5}{T_2} = \frac{p_5}{p_2} = 1 \tag{B-8d}$$

The location of the interface between regions 3 and 5, in the vicinity of the wall, is denoted I in Fig. 6. Point I represents a stagnation point between the flow in regions 3 and 5, when these flows are viewed in a point I stationary coordinate system. The static pressures, stagnation pressures, and Mach numbers relative to point I are equal in regions 3 and 5. It then follows that

$$\frac{\bar{u}_I}{u_i} = \frac{\bar{u}_5/u_i}{1 + (\rho_3/\rho_5)^{1/2}} \tag{B-9a}$$

$$\frac{p_I}{p_3} = \left[1 + \frac{\gamma - 1}{2} \left(\frac{\bar{u}_I}{a_3}\right)^2\right]^{\gamma/(\gamma - 1)} \tag{B-9b}$$

where p_I is the local wall surface and $\bar{u}_I$ is the velocity of point I in point E stationary coordinates. Values of $\bar{u}_I$ and p_I are included in Table 3.

C. POINT F STATIONARY

Point F is defined as the intersection between the primary Mach stem m and the wall surface (Fig. 4). The coordinate system considered herein assumes point F is stationary, whereas the free-stream, wall, and triple-point have motion. The present coordinate system is denoted by the symbol (~) and is useful for analysis of the boundary layer in region 3.

Velocities in the F-stationary coordinate system are obtained by subtracting the Mach stem velocity $\bar{u}_m$ in the E-stationary system from velocities therein. The results are

$$\frac{\tilde{u}_w}{u_i} = \frac{\tilde{u}_0}{u_i} = \frac{\cos\psi}{\cos(\theta + \psi)} \tag{B-10a}$$

$$\frac{\tilde{u}_E}{u_i} = \frac{\tilde{u}_3}{u_i} = \frac{1}{K_1} \frac{\cos\psi}{\cos(\theta + \psi)} \tag{B-10b}$$

$$\frac{\tilde{u}_T}{u_i} = \frac{u_3}{u_i} \cos\alpha \tag{B-10c}$$

$$\frac{\tilde{u}_2}{u_i} = \left[\left(\frac{\bar{u}_2}{u_i} \sin\alpha + \frac{\bar{u}_m}{u_i}\right)^2 + \left(\frac{\bar{u}_2}{u_i} \cos\alpha\right)^2\right]^{1/2} \tag{B-10d}$$

$$\frac{\tilde{u}_4}{u_i} = \left[\left(\frac{\bar{u}_4}{u_i} \sin\alpha + \frac{\bar{u}_m}{u_i}\right)^2 + \left(\frac{\bar{u}_4}{u_i} \cos\alpha\right)^2\right]^{1/2} \tag{B-10e}$$

$$\frac{\tilde{u}_5}{u_i} = \frac{\bar{u}_5}{u_i} - \frac{\bar{u}_m}{u_i} \tag{B-10f}$$

Values are listed in Table 3.

APPENDIX C. REGULAR REFLECTION

The flow field in regions 0, 1, and 2 is evaluated herein for the case of a strong incident shock and regular reflection. The coordinate system considered is the one wherein the point T (now a point of regular reflection) is stationary (Fig. 4).

The equations derived in Appendix B for regions 0, 1, and 2 are applicable, subject to the boundary condition that the flow in region 2 be tangent to the wedge surface. The angle α is now viewed as the angle between the stream lines in region 2 and the normal to the wedge surface. It follows that

$$\alpha = \pi/2 \tag{C-1a}$$

$$\delta = (\pi/2) - \theta - \beta \tag{C-1b}$$

For given values of γ and θ, the quantities β and M_1 are found from Eqs. (B-2a) and (B-b). The pressure ratio ξ is then found from Eq. (B-4c) by iteration, and all other quantities of interest can be evaluated from expressions for regions 1 and 2 in Appendix B. [Note that Eq. (B-4b) is not applicable.] Numerical results are presented in Table 2. The minimum value of θ therein corresponds to the condition for oblique shock detachment from the equivalent wedge δ. The latter value of θ is denoted θ_D and is usually considered the value of θ at which the transition from regular to Mach reflection occurs. Values of θ_D are found by replacing Eq. (B-4c) by the shock detachment condition (e.g., Ref. 6)

$$\xi = \frac{(\gamma + 1)(M_1^2 - 2) + \{(\gamma + 1)[(\gamma + 1)M_1^4 + 8(\gamma - 1)M_1^2 + 16]\}^{1/2}}{2(\gamma + 1)} \tag{C-2}$$

and are given in Table 2.

APPENDIX D. HEIGHT-OF-BURST FLOW FIELD

The interaction between an altitude burst and a ground plane is investigated for the case of a strong shock and an ideal gas (see Fig. 3). Blast wave properties are first noted. The reflection of the blast wave by the ground is then deduced. It is assumed that the reflection is similar, at each instant, to the reflection of a strong shock by a wedge. The results of Appendixes B and C are then applicable.

A. BLAST WAVE PROPERTIES

Consider a point source of energy E to detonate at a height h above a plane surface (see Fig. 3). The blast wave radius is denoted R and the pressure directly behind the wave is denoted p_1. For the case of a strong blast wave and an ideal gas, the flow field is self-similar at each instant[7] (excluding ground effect). The quantities E, p_1, and R are related by

$$p_1 = B\ E/R^3 \tag{D-1a}$$

where B is a nondimensional function of γ and has the values B = 0.12, 0.157, and 0.243 for γ = 9/7, 7/5, and 5/3. In mixed engineering units, Eq. (D-1a) can be expressed*

$$p_1(\mathrm{ATM}) = \frac{1.46\ B\ E(\mathrm{KT})}{[R(\mathrm{KFT})]^3} \tag{D-1b}$$

Equation (D-1) defines the pressure directly behind the shock for those portions of the blast wave that are uninfluenced by the ground.

*Equation (D-1b), with γ = 7/5, agrees to within 2% with an expression deduced by . . L. Brode for strong blast waves in air.[8]

Eq. (D-1a) can be generalized to include planar ($\sigma = 0$), cylindrical ($\sigma = 1$), and spherical blast waves. The result is[7]

$$p_1 = BE/R^{1+\sigma} \tag{D-1c}$$

where $B = 0.112$, 0.212, and 0.340 for $\gamma = 1.2$, 1.4, and 5/3, and $\sigma = 1$. In the case of a symmetric planar blast ($\sigma = 0$, $-R < r < R$), $B = 0.180$, 0.344, and 0.550 for $\gamma = 1.2$, 1.4, and 5/3. Flow properties vary with distance behind the shock. A linear approximation to flow properties at radius r, near the shock, is

$$\frac{R}{p_1}\,\frac{p - p_1}{r - R} = \frac{(2\gamma - 1)(\sigma + 1)}{\gamma - 1} - \frac{2\gamma\sigma}{\gamma + 1} \tag{D-1d}$$

$$\frac{R}{\rho_1}\,\frac{\rho - \rho_1}{r - R} = \frac{3(\sigma + 1)}{\gamma - 1} - \frac{2\sigma}{\gamma + 1} \tag{D-1e}$$

$$\frac{R}{u}\,\frac{u - u_1}{r - R} = \frac{3(\sigma + 1)}{2} - \frac{2\gamma\sigma}{\gamma + 1} \tag{D-1f}$$

where subscript 1 denotes properties directly behind the shock.

B. GROUND REFLECTION

The reflection of the blast wave by the ground is now considered. Let x denote ground range from the point of explosion, and let y_t denote the corresponding height of the triple point in the Mach reflection region. The angle between the normal to the shock (at the triple point) and the ground is (see Fig. 3)

$$\theta = \cot^{-1}\left[\frac{x/h}{1 - (y_t/h)}\right] \tag{D-2}$$

Equation (D-2), with $y_t = 0$, applies in the regular reflection region (i.e., $\theta > \theta_D$). The slope of the triple-point trajectory is (see Fig. 3)

$$\frac{dy_t}{dx} = \tan\psi \tag{D-3}$$

If Eq. (D-3) is substituted into the differential of Eq. (D-2) and the result is integrated, it is found that, for $\theta > \theta_D$ and $\theta < \theta_D$, respectively,

$$\frac{y_t}{h} = 0 \tag{D-4a}$$

$$= 1 - \exp \int_{\theta_D}^{\theta} \frac{\tan\psi \, d\theta}{\sin^2\theta(1 + \tan\psi \cot\theta)} \tag{D-4b}$$

Equation (D-4b) can be integrated if ψ is a known function of θ. It is assumed herein that the relation between ψ and θ is the same as that for shock passage over a wedge, as given in Appendixes B and C (i.e., a local similarity assumption). Equations (D-2) and (D-4) are then parametric equations that relate θ, x/h, and y_t/h. Corresponding values for $\gamma = 9/7$, $7/5$, and $5/3$ are given in Table 4. The triple-point trajectory, y_t/h versus x/h, is illustrated in Fig. 8.

The pressure behind the incident shock at the triple point is

$$\frac{h^3 p_1}{EB} = \frac{h^3}{R^3} = \left(\frac{\sin\theta}{1 - (y_t/h)}\right)^3 \tag{D-5a}$$

The surface pressures in the regular and Mach reflection region can be found from the expression

$$\frac{h^3 p_*}{EB} = \left(\frac{\sin\theta}{1 - (y_t/h)}\right)^3 \frac{p_*}{p_1} \qquad \text{(D-5b)}$$

where $p_* \equiv p_2$, p_3, or $p_{s,4}$, and p_*/p_1 is a function of γ and θ that is found from Appendixes B or C. Values of p_*/p_1 are included in Table 4. The corresponding value of p_1 for a ground burst ($h = 0$) is denoted $(p_1)_{GB}$ and is found from

$$\frac{1}{2}\left(\frac{h^3 p_1}{EB}\right)_{GB} = \left(\frac{h}{x}\right)^3 = \left(\frac{\tan\theta}{1 - (y_t/h)}\right)^3 \qquad \text{(D-5c)}$$

which is also included in Table 4. The coefficient 1/2 appears in Eq. (D-5c) because the effective energy of the ground burst is 2E. The variation of surface pressure with ground range is illustrated in Fig. 9. Comparison with $(p_1)_{GB}$ indicates the relative effectiveness of ground and altitude bursts with regard to induced surface pressure.

ADDENDUM: NUMERICAL RESULTS FOR $\gamma = 6/5$

Tables 1, 3, and 4 have been expanded to include the case $\gamma = 6/5$. These results are included herein.

Table 1. Regular Reflection for the Case of Strong Incident Shock and Ideal Gas

γ	β	M_1	θ	$\frac{\rho_1}{\rho_0}$	$\frac{p_1}{M_1^2 p_0}$	M_2	δ	ω	$\frac{\rho_2}{\rho_1}$	$\frac{p_2}{p_1}$
6/5	90.00	∞	0.00	11.00	1.09	∞	0.00	0.00	5.95	12.75
	85.00	36.30	0.46	11.00	1.09	24.59	4.54	0.92	5.98	12.92
	80.00	18.01	0.92	11.00	1.09	12.10	9.08	1.87	5.93	12.68
	75.00	11.85	1.40	11.00	1.09	7.85	13.60	2.90	5.85	12.28
	73.31	10.59	1.56	11.00	1.09	6.97	15.13	3.28	5.81	12.12
	70.00	8.73	1.90	11.00	1.09	5.66	18.10	4.07	5.73	11.75
	65.00	6.82	2.43	11.00	1.09	4.28	22.57	5.46	5.57	11.10
	60.00	5.51	3.00	11.00	1.09	3.31	27.00	7.19	5.38	10.36
	55.00	4.54	3.64	11.00	1.09	2.56	31.36	9.52	5.16	9.56
	50.00	3.80	4.36	11.00	1.09	1.93	35.64	12.97	4.93	8.75
	45.00	3.19	5.19	11.00	1.09	1.31	39.81	19.79	4.74	8.16
	43.54	3.03	5.46	11.00	1.09	0.95	40.99	27.24	4.86	8.56

Table 3. Mach Reflection for the Case of Strong Shock and Ideal Gas, $\gamma = 6/5$

		Region 1				Region 2				
α	θ	M_1	β	$\frac{\rho_1}{\rho_0}$	$\frac{P_1}{M_1^2 P_0}$	M_2	χ	ω	$\frac{\rho_2}{\rho_1}$	$\frac{P_2}{P_1}$
73.306	0.000	10.592	1.562	11.000	1.091	6.970	15.132	3.279	5.809	12.119
72.500	0.073	10.120	1.635	11.000	1.091	6.803	15.063	3.429	5.582	11.749
70.000	0.301	8.874	1.864	11.000	1.091	6.309	14.832	3.935	4.940	8.801
67.500	0.531	7.877	2.100	11.000	1.091	5.851	14.574	4.509	4.387	7.145
65.000	0.766	7.060	2.343	11.000	1.091	5.429	14.289	5.154	3.914	5.934
62.500	1.006	6.377	2.595	11.000	1.091	5.041	13.978	5.870	3.511	5.023
60.000	1.251	5.795	2.855	11.000	1.091	4.685	13.641	6.662	3.167	4.321
57.500	1.503	5.293	3.126	11.000	1.091	4.359	13.279	7.534	2.874	3.768
55.000	1.762	4.854	3.409	11.000	1.091	4.059	12.892	8.488	2.623	3.325
52.500	2.031	4.466	3.706	11.000	1.091	3.783	12.482	9.531	2.408	2.966
50.000	2.311	4.120	4.018	11.000	1.091	3.528	12.048	10.669	2.222	2.671
47.500	2.602	3.809	4.346	11.000	1.091	3.291	11.591	11.908	2.062	2.426
45.000	2.908	3.527	4.695	11.000	1.091	3.072	11.113	13.257	1.923	2.220
43.544	3.093	3.375	4.907	11.000	1.091	2.951	10.824	14.098	1.850	2.115
42.500	3.229	3.270	5.065	11.000	1.091	2.868	10.612	14.727	1.802	2.046
40.000	3.569	3.034	5.459	11.000	1.091	2.677	10.090	16.328	1.696	1.897
37.500	3.929	2.817	5.881	11.000	1.091	2.499	9.548	18.076	1.603	1.770
35.000	4.313	2.616	6.335	11.000	1.091	2.331	8.984	19.989	1.522	1.661
32.500	4.725	2.430	6.824	11.000	1.091	2.175	8.399	22.086	1.451	1.566
30.000	5.168	2.256	7.352	11.000	1.091	2.027	7.793	24.392	1.388	1.484
27.500	5.648	2.094	7.925	11.000	1.091	1.889	7.165	26.939	1.332	1.413
25.000	6.170	1.942	8.547	11.000	1.091	1.759	6.515	29.763	1.284	1.350
22.500	6.741	1.801	9.224	11.000	1.091	1.637	5.841	32.909	1.240	1.295
20.000	7.369	1.669	9.960	11.000	1.091	1.523	5.143	36.429	1.202	1.247
17.500	8.066	1.546	10.760	11.000	1.091	1.418	4.421	40.391	1.168	1.205
15.000	8.842	1.433	11.624	11.000	1.091	1.321	3.677	44.871	1.137	1.167
12.500	9.717	1.329	12.548	11.000	1.091	1.234	2.916	49.964	1.110	1.134
10.000	10.710	1.235	13.520	11.000	1.091	1.156	2.151	55.780	1.085	1.103
7.500	11.854	1.152	14.511	11.000	1.091	1.091	1.408	62.448	1.063	1.076
5.000	13.189	1.083	15.466	11.000	1.091	1.040	0.737	70.134	1.042	1.050
2.500	14.785	1.029	16.285	11.000	1.091	1.007	0.220	79.092	1.021	1.025
1.000	15.918	1.008	16.641	11.000	1.091	0.999	0.040	85.308	1.009	1.010

Table 3. Mach Reflection for the Case of Strong Shock and Ideal Gas, $\gamma = 6/5$ (Continued)

		Region 3				Region 4			
			$\frac{\rho_3}{\rho_0}$	$\frac{p_3}{\eta_1^2 p_0}$	$\bar{\eta}_3$	$\frac{\rho_4}{\rho_2}$	$\frac{p_4}{p_2}$	$\frac{p_{s,4}}{p_3}$	$\frac{p_4}{p_1}$
[illegible]	[illegible]	[illegible]	[illegible]	[illegible]	[illegible]	[illegible]	[illegible]	[illegible]	[illegible]
[illegible]	.289	90.000	11.000	13.220	5.274	8.772	42.850	45.614	519.285
[illegible]	.289	89.196	11.000	12.162	5.121	8.683	40.786	43.445	454.714
[illegible]	.289	86.697	11.000	9.601	5.667	8.388	34.940	37.301	307.496
[illegible]	.290	84.174	11.000	7.794	5.243	8.066	29.901	32.005	213.635
[illegible]	.292	81.632	11.000	6.474	4.852	7.720	25.586	27.471	151.837
[illegible]	.294	79.072	11.000	5.480	4.490	7.353	21.903	23.601	110.025
[illegible]	.297	76.496	11.000	4.713	4.157	6.968	18.761	20.299	81.059
[illegible]	.300	73.905	11.000	4.110	3.850	6.568	16.077	17.479	60.573
[illegible]	.305	71.302	11.000	3.628	3.566	6.157	13.778	15.064	45.817
[illegible]	.311	68.688	11.000	3.236	3.302	5.738	11.804	12.991	35.013
[illegible]	.316	66.066	11.000	2.914	3.057	5.314	10.103	11.205	26.985
[illegible]	.323	63.438	11.000	2.646	2.828	4.888	8.634	9.663	20.941
[illegible]	.331	60.807	11.000	2.422	2.613	4.464	7.360	8.327	16.338
[illegible]	.336	59.275	11.000	2.307	2.494	4.219	6.697	[illegible]	[illegible]
[illegible]	.340	58.177	11.000	2.232	2.412	4.045	6.254	7.168	12.794
[illegible]	.350	55.550	11.000	2.079	2.221	3.634	5.291	[illegible]	[illegible]
37.500	0.362	52.929	11.000	1.931	2.041	3.234	4.451	5.282	7.881
35.000	0.375	50.319	11.000	1.812	1.869	2.847	3.719	4.518	6.177
32.500	0.390	47.722	11.000	1.709	1.705	2.477	3.079	3.854	4.823
30.000	0.407	45.145	11.000	1.619	1.547	2.125	2.521	3.278	3.743
27.500	0.427	42.590	11.000	1.541	1.396	1.795	2.038	2.781	2.876
25.000	0.449	40.061	11.000	1.473	1.251	1.488	1.615	2.358	2.181
22.500	0.474	37.565	11.000	1.413	1.110	1.206	1.252	2.004	1.622
20.000	0.502	35.103	11.000	1.361	0.973	1.000	1.000	1.721	1.247
17.500	0.535	32.681	11.000	1.314	0.840	1.000	1.000	1.506	1.205
15.000	0.572	30.301	11.000	1.273	0.711	1.000	1.000	1.344	1.167
12.500	0.616	27.964	11.000	1.237	0.585	1.000	1.000	1.224	1.134
10.000	0.666	25.671	11.000	1.204	0.462	1.000	1.000	1.135	1.103
7.500	0.726	23.419	11.000	1.174	0.342	1.000	1.000	1.072	1.076
5.000	0.798	21.202	11.000	1.148	0.225	1.000	1.000	1.031	1.050
2.500	0.886	19.006	11.000	1.119	0.111	1.000	1.000	1.007	1.025
1.000	0.950	17.681	11.000	1.102	0.044	1.000	1.000	1.001	1.010

Table 3. Mach Reflection for the Case of Strong Shock and Ideal Gas, $\gamma = 6/5$ (Continued)

	Region 5				Interfaces				
θ	$\frac{q_5}{q_1}$	$\frac{\rho_5}{\rho_1}$	$\frac{u_5}{u_1}$	$\frac{v_5}{u_1}$	$\frac{q_2}{q_1}$	$\frac{p_2}{p_1}$	$\frac{u_2}{u_1}$	$\frac{v_2}{u_1}$	$\frac{v_2}{u_1}$
73.500	2.984	2.611	0.467	0.171	1.225	1.077	0.316	3.165	3.481
72.500	2.958	2.532	0.497	0.194	1.294	1.087	0.304	3.035	3.339
71.500	2.877	2.304	0.523	0.254	1.497	1.117	0.279	2.697	2.967
67.500	2.796	2.104	0.544	0.301	1.685	1.151	0.263	2.430	2.673
66.500	2.715	1.931	0.562	0.341	1.861	1.186	0.221	2.215	2.436
62.500	2.634	1.781	0.578	0.374	2.025	1.223	0.204	2.037	2.241
60.000	2.553	1.652	0.592	0.403	2.179	1.262	0.189	1.890	2.079
57.500	2.472	1.541	0.605	0.429	2.324	1.302	0.176	1.765	1.941
55.000	2.391	1.445	0.618	0.452	2.462	1.344	0.166	1.658	1.824
52.500	2.309	1.363	0.630	0.474	2.594	1.387	0.157	1.566	1.722
50.000	2.227	1.293	0.643	0.494	2.722	1.433	0.149	1.486	1.634
47.500	2.143	1.233	0.656	0.514	2.846	1.480	0.142	1.416	1.557
45.000	2.058	1.182	0.669	0.533	2.968	1.529	0.135	1.354	1.490
43.500	2.016	1.156	0.676	0.544	3.038	1.560	0.132	1.322	1.454
42.500	1.971	1.139	0.682	0.552	3.087	1.582	0.130	1.300	1.430
41.000	1.881	1.103	0.695	0.570	3.206	1.637	0.125	1.252	1.377
37.500	1.788	1.073	0.708	0.587	3.323	1.696	0.121	1.21	1.331
35.000	1.690	1.049	0.722	0.604	3.438	1.757	0.117	1.172	1.289
32.500	1.588	1.031	0.734	0.620	3.549	1.820	0.114	1.138	1.252
30.000	1.479	1.017	0.745	0.634	3.653	1.883	0.111	1.108	1.218
27.500	1.363	1.008	0.754	0.646	3.745	1.941	0.108	1.081	1.189
25.000	1.240	1.002	0.759	0.653	3.818	1.989	0.106	1.056	1.162
22.500	1.108	1.000	0.758	0.655	3.863	2.020	0.103	1.035	1.138
20.000	0.973	1.000	0.753	0.652	3.880	2.032	0.102	1.015	1.117
17.500	0.840	1.000	0.747	0.647	3.886	2.037	0.100	0.998	1.098
15.000	0.711	1.000	0.739	0.641	3.886	2.036	0.098	0.982	1.080
12.500	0.585	1.000	0.732	0.635	3.879	2.031	0.097	0.968	1.065
10.000	0.462	1.000	0.724	0.628	3.867	2.023	0.095	0.955	1.050
7.500	0.342	1.000	0.715	0.621	3.851	2.012	0.094	0.943	1.037
5.000	0.225	1.000	0.707	0.614	3.832	1.999	0.093	0.932	1.025
2.500	0.111	1.000	0.697	0.605	3.807	1.982	0.092	0.921	1.013
1.000	0.044	1.000	0.691	0.599	3.787	1.969	0.091	0.914	1.005

Table 4. Variation of Pressure with Range for Height-of-Burst Case

	$\frac{x}{h}$		$\frac{1}{2}\left(\frac{h^3 p_1}{BE}\right)_{GB}$	$\frac{h^3 p_1}{BE}$	$\frac{h^3 p_2}{BE}$
[illegible]	0.30	90.00	[illegible]	1.00	12.75
	0.39	85.00	1493.29	0.99	12.77
	0.18	80.00	282.41	0.96	12.11
	0.27	75.00	51.98	0.90	11.07
	0.36	70.00	20.74	0.83	9.75
	0.47	65.00	9.86	0.74	8.26
	0.58	60.00	5.20	0.65	6.73
	0.70	55.00	2.91	0.55	5.25
	0.84	50.00	1.69	0.45	3.93
	1.00	45.00	1.00	0.35	2.88
	1.05	43.54	0.86	0.33	2.80

(b) Mach Reflection Regime

	$\frac{x}{h}$	$\frac{v_m}{h}$		$\frac{1}{2}\left(\frac{h^3 p_1}{BE}\right)_{GB}$	$\frac{h^3 p_1}{BE}$	$\frac{h^3 p_3}{BE}$	$\frac{h^3 p_{s,4}}{BE}$
[illegible]	1.052	0.000	43.544	0.859	0.327	0.691	0.278
	1.089	0.002	42.500	0.774	0.310	0.635	0.549
	1.183	0.008	40.000	0.604	0.272	0.516	3.179
	1.285	0.014	37.500	0.472	0.236	0.417	2.203
	1.396	0.022	35.000	0.367	0.202	0.335	1.515
	1.519	0.032	32.500	0.285	0.171	0.268	1.033
	1.656	0.044	30.000	0.220	0.143	0.212	0.696
	1.809	0.058	27.500	0.169	0.118	0.167	0.463
	1.981	0.076	25.000	0.129	0.096	0.129	0.305
	2.177	0.098	22.500	0.097	0.076	0.099	0.199
	2.401	0.126	20.000	0.072	0.060	0.075	0.129
	2.660	0.161	17.500	0.053	0.046	0.056	0.084
	2.962	0.206	15.000	0.038	0.035	0.040	0.054
	3.318	0.264	12.500	0.027	0.025	0.029	0.035
	3.740	0.341	10.000	0.019	0.018	0.020	0.023
	4.244	0.441	7.500	0.013	0.013	0.014	0.015
	4.848	0.576	5.000	0.009	0.009	0.009	0.009
	5.573	0.757	2.500	0.006	0.006	0.006	0.006
	6.073	0.894	1.000	0.004	0.004	0.005	0.005

LABORATORY OPERATIONS

The Laboratory Operations of The Aerospace Corporation is conducting experimental and theoretical investigations necessary for the evaluation and application of scientific advances to new military space systems. Versatility and flexibility have been developed to a high degree by the laboratory personnel in dealing with the many problems encountered in the nation's rapidly developing space systems. Expertise in the latest scientific developments is vital to the accomplishment of tasks related to these problems. The laboratories that contribute to this research are:

Aerophysics Laboratory: Launch vehicle and reentry aerodynamics and heat transfer, propulsion chemistry and fluid mechanics, structural mechanics, flight dynamics; high-temperature thermomechanics, gas kinetics and radiation; research in environmental chemistry and contamination; cw and pulsed chemical laser development including chemical kinetics, spectroscopy, optical resonators and beam pointing, atmospheric propagation, laser effects and countermeasures.

Chemistry and Physics Laboratory: Atmospheric chemical reactions, atmospheric optics, light scattering, state-specific chemical reactions and radiation transport in rocket plumes, applied laser spectroscopy, laser chemistry, battery electrochemistry, space vacuum and radiation effects on materials, lubrication and surface phenomena, thermionic emission, photosensitive materials and detectors, atomic frequency standards, and bioenvironmental research and monitoring.

Electronics Research Laboratory: Microelectronics, GaAs low-noise and power devices, semiconductor lasers, electromagnetic and optical propagation phenomena, quantum electronics, laser communications, lidar, and electro-optics; communication sciences, applied electronics, semiconductor crystal and device physics, radiometric imaging; millimeter-wave and microwave technology.

Information Sciences Research Office: Program verification, program translation, performance-sensitive system design, distributed architectures for spaceborne computers, fault-tolerant computer systems, artificial intelligence, and microelectronics applications.

Materials Sciences Laboratory: Development of new materials: metal matrix composites, polymers, and new forms of carbon; component failure analysis and reliability; fracture mechanics and stress corrosion; evaluation of materials in space environment; materials performance in space transportation systems; analysis of systems vulnerability and survivability in enemy-induced environments.

Space Sciences Laboratory: Atmospheric and ionospheric physics, radiation from the atmosphere, density and composition of the upper atmosphere, aurorae and airglow; magnetospheric physics, cosmic rays, generation and propagation of plasma waves in the magnetosphere; solar physics, infrared astronomy; the effects of nuclear explosions, magnetic storms, and solar activity on the earth's atmosphere, ionosphere, and magnetosphere; the effects of optical, electromagnetic, and particulate radiations in space on space systems.

END

DATE
FILMED

9 — 83

DTIC